OXFORD GENETICS

Reduced histone gene copy number disrupts *Drosophila* Polycomb function

Jeanne-Marie E. McPherson,[1,2] Lucy C. Grossmann,[3] Harmony R. Salzler,[3,2] Robin L. Armstrong,[1,2] Esther Kwon,[3]
A. Gregory Matera,[1,3,2,4,5] Daniel J. McKay,[1,3,2,4,*] Robert J. Duronio [1,3,2,4,5,*]

[1]Curriculum in Genetics and Molecular Biology, University of North Carolina, Chapel Hill, NC, 27599 USA
[2]Integrative Program for Biological and Genome Sciences, University of North Carolina, Chapel Hill, NC, 27599, USA
[3]Department of Biology, University of North Carolina, Chapel Hill, NC, 27599, USA
[4]Department of Genetics, University of North Carolina, Chapel Hill, NC, 27599, USA
[5]Lineberger Comprehensive Cancer Center, University of North Carolina, Chapel Hill, NC, 27599, USA

*Corresponding author: Email: dmckay1@email.unc.edu; *Corresponding author: Email: duronio@med.unc.edu

Abstract

The chromatin of animal cells contains two types of histones: canonical histones that are expressed during S phase of the cell cycle to package the newly replicated genome, and variant histones with specialized functions that are expressed throughout the cell cycle and in non-proliferating cells. Determining whether and how canonical and variant histones cooperate to regulate genome function is integral to understanding how chromatin-based processes affect normal and pathological development. Here, we demonstrate that variant histone H3.3 is essential for *Drosophila* development only when canonical histone gene copy number is reduced, suggesting that coordination between canonical *H3.2* and variant *H3.3* expression is necessary to provide sufficient H3 protein for normal genome function. To identify genes that depend upon, or are involved in, this coordinate regulation we screened for heterozygous chromosome 3 deficiencies that impair development of flies bearing reduced *H3.2* and *H3.3* gene copy number. We identified two regions of chromosome 3 that conferred this phenotype, one of which contains the *Polycomb* gene, which is necessary for establishing domains of facultative chromatin that repress master regulator genes during development. We further found that reduction in *Polycomb* dosage decreases viability of animals with no *H3.3* gene copies. Moreover, heterozygous *Polycomb* mutations result in de-repression of the Polycomb target gene *Ubx* and cause ectopic sex combs when either canonical or variant *H3* gene copy number is reduced. We conclude that Polycomb-mediated facultative heterochromatin function is compromised when canonical and variant *H3* gene copy number falls below a critical threshold.

Keywords: *Drosophila melanogaster*, chromatin, development, canonical histone, variant histone, Polycomb

Introduction

To control access to information encoded in the genome, eukaryotes organize their DNA into chromatin, which regulates all DNA-dependent processes including transcription, DNA replication, and DNA damage repair (Allis *et al.* 2007; Kornberg and Lorch 2020). The fundamental unit of chromatin is a nucleosome composed of approximately 147 bp of DNA wrapped around a histone octamer containing two copies of each of the four core histones: H2A, H2B, H3, and H4 (Luger *et al.* 1997). Tight control over histone levels is essential for normal genome function. For instance, mutations in *abo* and *mute*—which negatively regulate histone mRNA levels—reduce viability in *Drosophila melanogaster* (Berloco *et al.* 2001; Bulchand *et al.* 2010). In budding yeast, mutations that cause an accumulation of excess histone proteins result in impaired growth, DNA damage sensitivity, and chromosome loss (Meeks-Wagner and Hartwell 1986; Gunjan and Verreault 2003). Conversely, conditional repression of histone transcription during S phase impairs DNA replication and causes cell cycle arrest in yeast and fruit flies (Han *et al.* 1987; Sullivan *et al.* 2001; Gossett and Lieb 2012). Similarly, deletion of all *D. melanogaster* canonical histone genes leads to cell cycle arrest and embryonic

lethality (Smith *et al.* 1993; Günesdogan *et al.* 2010; McKay *et al.* 2015). Histone chaperone mutations that reduce incorporation of histone proteins into chromatin cause spurious transcription, chromosome segregation defects, chromosomal rearrangements, and enhanced DNA damage (Clark-Adams *et al.* 1988; Nelson *et al.* 2002; Myung *et al.* 2003; Ye *et al.* 2003; Nashun *et al.* 2015; Mühlen *et al.* 2023). For these reasons, precise regulation of histone mRNA and protein levels is critical for normal cell function and development, yet we have an incomplete understanding of the mechanisms involved.

Most research investigating the mechanisms of histone expression has focused on the canonical histone genes, which are synthesized in large amounts during S phase to properly package newly replicated DNA into chromatin. This work provides evidence supporting regulation at both the transcriptional and post-transcriptional levels (Marzluff and Duronio 2002; Duronio and Marzluff 2017). For example, in Chinese hamster ovary cells, canonical histone mRNA levels increase 35-fold as cells enter S phase (Harris *et al.* 1991). As cells exit S phase, canonical histone transcription is terminated and the corresponding mRNAs are rapidly degraded (Kaygun and Marzluff 2005; Eriksson *et al.*

2012). Coordinate expression among histone genes to maintain nucleosome subunit stoichiometry is also important; this requirement is reflected in the clustered arrangement and co-regulation of the canonical histone genes in multiple species, including *D. melanogaster,* yeast, and mammals (Lifton *et al.* 1977; Smith and Murray 1983; Eriksson *et al.* 2012). In the *D. melanogaster* histone gene complex (*HisC*, Fig. 1a), *H2A* and *H2B* share a bidirectional promoter, as do *H3* and *H4* (Lifton *et al.* 1977). Histone protein levels are also controlled post-translationally. For example, yeast histones that are not chromatin-bound are rapidly degraded, suggesting that excess histone proteins are deleterious to cell function (Singh *et al.* 2009). Another example of post-translational control that applies to a variant histone occurs during *Drosophila* oogenesis when the pool of free H2Av protein is regulated by Jabba, which physically sequesters H2Av to prevent its degradation (Stephenson *et al.* 2021).

Whereas canonical histones are encoded by multiple genes that are expressed exclusively during S phase of the cell cycle (Fig. 1, a and b), an additional layer of complexity is provided by the expression of cell cycle independent histones (Franklin and Zweidler 1977; Verreault *et al.* 1996; Marzluff *et al.* 2002; Tagami *et al.* 2004). These so-called "variant" histones are typically encoded by one or two genes and are expressed throughout the cell cycle (Fig. 1, a and b) (Urban and Zweidler 1983; Pantazis and Bonner 1984; Zweidler 1984; Brown *et al.* 1985; Piña and Suau 1987; Wunsch and Lough 1987; McKittrick *et al.* 2004; Tagami *et al.* 2004; Mito *et al.* 2005; Szenker *et al.* 2011; Maze *et al.* 2015; Tvardovskiy *et al.* 2017; Sauer *et al.* 2018). The tight control of canonical histone levels and the severe negative impact of histone mis-expression raises the possibility that coordinate regulation between canonical and variant histones is important for genome function and stability. For instance, in the early *Drosophila* embryo an increase in the ratio of variant H2Av to canonical H2A causes mitotic defects and reduces viability (Li *et al.* 2014). Here, we address the question of coordinate regulation between variant and canonical histone genes by focusing on those encoding histone H3.

In *D. melanogaster*, the non-centromeric H3 variant is encoded by two genes that produce identical proteins, *H3.3A* and *H3.3B* (Fig. 1a). Variant H3.3 differs from canonical H3.2 by only four amino acid residues (Fig. 1c), and these differences are highly conserved among other animals including humans (Malik and Henikoff 2003; Szenker *et al.* 2011). Three of the four residues are found in the globular domain and are known to modulate interactions with the histone chaperone complexes that deposit histones into chromatin (Grover *et al.* 2018). Canonical H3.2 is deposited during DNA replication by CAF-1 (chromatin assembly factor 1 complex) (Smith and Stillman 1989; Verreault *et al.* 1996; Shibahara and Stillman 1999; Tagami *et al.* 2004; Sauer *et al.* 2018). Variant H3.3 is deposited into chromatin by the ATRX (alpha-thalassemia X-linked mental retardation protein) complex and the HIRA (histone cell cycle regulator) complex (Ahmad and Henikoff 2002; Tagami *et al.* 2004; Schneiderman *et al.* 2009; Goldberg *et al.* 2010; Lewis *et al.* 2010; Rai *et al.* 2011; Orsi *et al.* 2013; Ray-Gallet *et al.* 2018; Torné *et al.* 2020). Whereas H3.2 is deposited evenly genome-wide during replication, H3.3 is enriched at sites with high nucleosome turnover, including active regulatory elements, transcribed gene bodies, and pericentromeric regions (Ahmad and Henikoff 2002; McKittrick *et al.* 2004; Mito *et al.* 2005; Wirbelauer *et al.* 2005; Loyola and Almouzni 2007; Goldberg *et al.* 2010; Szenker *et al.* 2011; Martire and Banaszynski 2020). The fourth amino acid difference between H3.2 and H3.3 occurs at position 31 in the post-translationally modified N-terminal tail (Szenker *et al.* 2011). Position 31 is an alanine in H3.2 (H3.2A31)

and a serine in H3.3 (H3.3S31), which can be phosphorylated (Hake *et al.* 2005; Martire *et al.* 2019; Armache *et al.* 2020; Sitbon *et al.* 2020). Other residues on the N-terminal tails of H3.2 and H3.3 are also differentially enriched in post-translational modifications (PTMs), likely due to their differential localization in the genome. Relative to H3.2, H3.3 is enriched with PTMs associated with active chromatin (e.g. H3K4me3) and depleted in marks associated with inactive chromatin (e.g. H3K9me2) (McKittrick *et al.* 2004; Hödl and Basler 2012). Although the mechanisms regulating canonical and variant histone mRNA and protein levels are distinct, we do not know if and how these mechanisms are coordinated to supply the necessary amount of each histone isotype across the genome. Here, we use *D. melanogaster* to explore this question by examining the consequences of manipulating the relative number of canonical and variant *H3* genes.

Genetically manipulating histone gene copy number is challenging in many metazoans, including mice and humans, because canonical histones are encoded by multiple gene clusters located at distinct chromosomal locations (Marzluff and Duronio 2002). *D. melanogaster* is a powerful organism to investigate the effects of altering histone gene copy number because all ~100 haploid copies of the canonical histone genes are tandemly repeated (Fig. 1a) and can be removed with a single genetic deletion, *ΔHisC* (Günesdogan *et al.* 2010). The ability to manipulate histone genes in *D. melanogaster* led to the discovery that canonical histone gene copy number is a modifier of position effect variegation (PEV), a genetic phenomenon associated with heterochromatin. Heterozygosity of the histone locus results in suppression of PEV, suggesting that histone abundance contributes to maintenance of epigenetic silencing of H3K9me3-marked constitutive heterochromatin (Moore *et al.* 1979; Moore *et al.* 1983; Sinclair *et al.* 1983). The ability to manipulate histone gene copy number in *D. melanogaster* has been extended in recent years. Replacement of all ~200 copies (*200xWT*) of the canonical histone genes with a transgene containing 12 wild-type canonical histone gene repeat units (*12xHWT*, Fig. 1a) is sufficient to support development and provides a means of altering canonical histone gene copy number with precision (McKay *et al.* 2015).

Here, we report that *12xHWT* viability depends on expression of variant *H3.3* genes, whereas *200xWT* viability does not. This finding suggests that coordination of H3.2 and H3.3 protein levels is necessary for proper development when either *H3.2* or *H3.3* gene copy number is reduced. We conducted a screen to identify genes involved in the coordinated control of *H3.2* and *H3.3*. We identified a deficiency that uncovers *Yem*, a component of the HIRA histone chaperone complex, the function of which may be particularly important when *H3.2* gene copy number is reduced. Surprisingly, we also found that reduction of *Polycomb* (*Pc*) gene function decreases viability of flies that have reduced numbers of *H3.3* genes. Furthermore, we found that reductions in either *H3.2* or *H3.3* gene copy number disrupt Polycomb-mediated gene repression. Rather than *Pc* being involved in the coordinate expression of canonical and variant H3, we conclude from these findings that the appropriate balance of *H3.2* and *H3.3* genes is critical for the proper epigenetic silencing of developmental genes and maintenance of facultative heterochromatin function.

Materials and methods
Fly stocks and husbandry
Fly stocks were maintained on standard corn medium provided by Archon Scientific (Durham, NC). See Supplementary Table 9 for a list of all stocks.
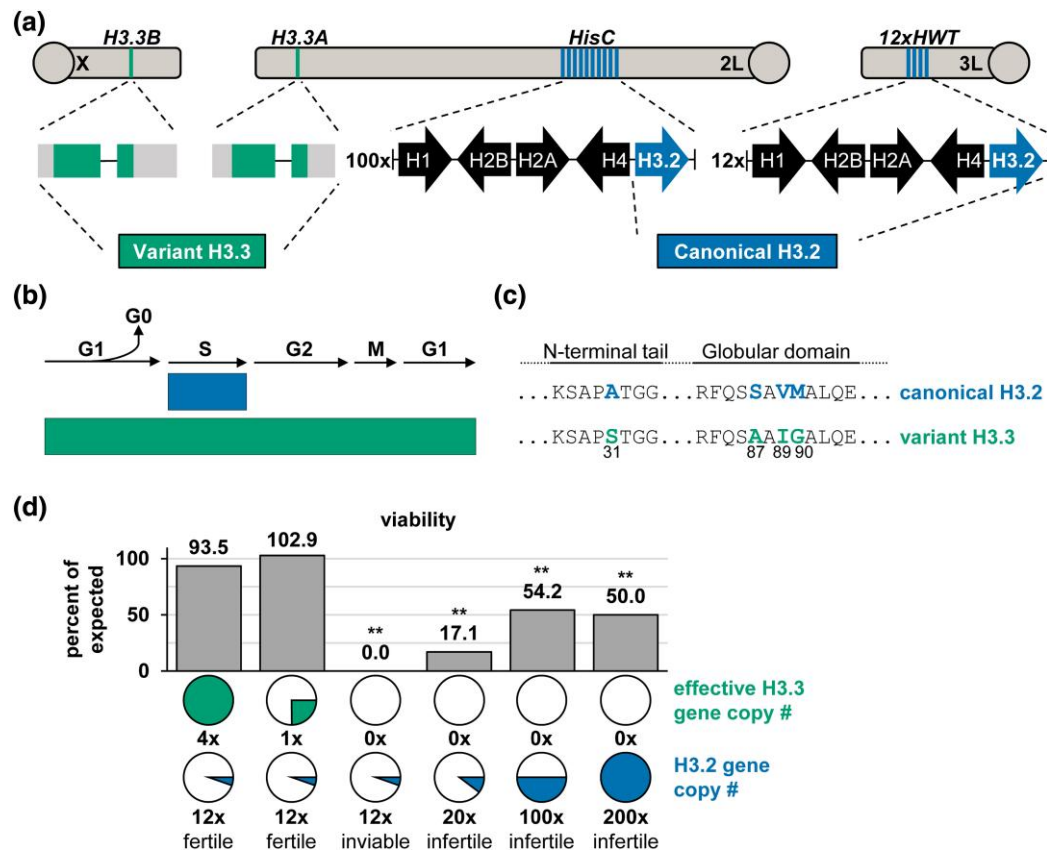
Fig. 1. *H3.3* is required for viability when *H3.2* gene copy number is reduced. a) Diagram of the genomic locations of the three H3 genes and the 12xHWT transgene. 100x and 12x indicate gene copy number. b) Schematic model of *H3.2* and *H3.3* expression during the cell cycle. c) Amino acid sequence differences of *H3.2* and *H3.3*. d) Bar plot of viability for the indicated genotypes. Circles represent the full complement of *H3.3* or *H3.2* gene copies present in the wild-type genome, and the color filling each circle (H3.3 green, H3.2 blue) indicates the number of gene copies present in each experimental genotype, e.g. A solid blue circle indicates the 200 *H3.2* gene copies of the diploid *HisC* locus. A solid green circle indicates 3 *H3.3* gene copies in males and 4 gene copies in females since *H3.3B* is on the X chromosome. The number of genes is shown below the circles, as well as whether surviving adults are fertile. Percent of expected genotypic frequencies based on Mendelian ratios. Asterisks indicate fewer than expected survive (chi-square test, ** $P < 0.01$, see Supplementary Table 1 for *P*-values).

CRISPR-mediated generation of *H3.3A^Δ*

pCFD4 plasmids encoding dual gRNAs (gRNA_1: caaggcgccccg-caagcagc, gRNA_2: tgcaccgtgactatttcata) targeting *H3.3A* were injected into embryos expressing Cas9 from the *nanos* promoter (*y1 M{nos-Cas9.P}ZH-2A w**; RRID: BDSC_54590) by *GenetiVision* Corporation (Houston, TX). *H3.3A^Δ* alleles were identified by PCR of genomic DNA and confirmed by sequencing, which revealed a 265 bp deletion removing amino acids 19 through 94 of the *H3.3A* open reading frame. The deletion breakpoints are indicated by "…/…" in the following sequence: CAAGGCGCCCCGCA…/…TACGGTCATGTAAT. The *H3.3A^Δ* allele was determined to be amorphic because *H3.3B^0*; *H3.3A^Δ*; *12xHWT/+* animals are inviable.

CRISPR diagnostic screen primer set: H3.3A^Δ for-CCCGATGAATATAGGGTCACAC, H3.3A^Δ rev-CTGGATGTCC TTGGGCATAAT. pCFD4-U6:1_U6:3 was a gift from Simon Bullock (Addgene plasmid #49411; http://n2t.net/addgene:49411; RRID:Addgene_49411). *His3.3A* reference sequence: NCBI Gene ID 33736.

Viability

To examine the effect of *H3.2* gene copy number on *H3.3^{null}* viability (Fig. 1d), the following four crosses were performed:

1) *H3.3B^0/H3.3B^0*; *H3.3A$^{2×1}$, ΔHisC, twistGal4/CyO*; x *yw/Y*; *H3.3$^{A2×1}$, ΔHisC, UAS-YFP/CyO; 12xHWT/12xHWT*;
2) *H3.3B^0/H3.3B^0*; *H3.3A$^{2×1}$, ΔHisC, twistGal4/CyO*; x *yw/Y*; *H3.3$^{A2×1}$, ΔHisC, UAS-YFP/CyO; 12xHWT-VK33, 8xHWT-86F6/+*;
3) *H3.3B^0/H3.3B^0*; *H3.3A$^{2×1}$, ΔHisC, twistGal4/CyO*; x *H3.3B^0/Y*; *H3.3A$^{2×1}$/CyO, twistGFP*; and
4) *H3.3B^0/H3.3B^0*; *H3.3A^Δ/CyO, twistGFP*; x *H3.3B^0/Y*; *H3.3A^Δ/CyO, twistGFP*.

To examine the effect of *H3.3* gene copy number on *12xHWT* viability (Fig. 1d), the following three crosses were performed:

1) *H3.3B^0/H3.3B^0*; *H3.3A$^{2×1}$, ΔHisC, UAS-YFP/CyO; 12xHWT/12xHWT* x *yw*; *H3.3$^{A2×1}$, ΔHisC^{Cadillac}/CyO*;
2) *yw/yw*; *H3.3A$^{2×1}$, ΔHisC^{Cadillac}; 12xHWT/12xHWT* x *H3.3B^0/Y*; *H3.3A$^{2×1}$, ΔHisC, twistGal4/CyO*; and
3) *yw/yw*; *ΔHisC, twistGal4/CyO*; x *yw*; *ΔHisC, UAS-YFP/CyO; 12xHWT/12xHWT*.

Vials were maintained at 25°C and flipped every other day. Data were plotted as percent observed of expected based on Mendelian ratios for each individual cross. Chi-squared analysis was performed to determine statistical significance. A significance threshold of $P < 0.05$ was used in this study. See Supplementary Table 1 for all genotypes and progeny numbers. All genotypes
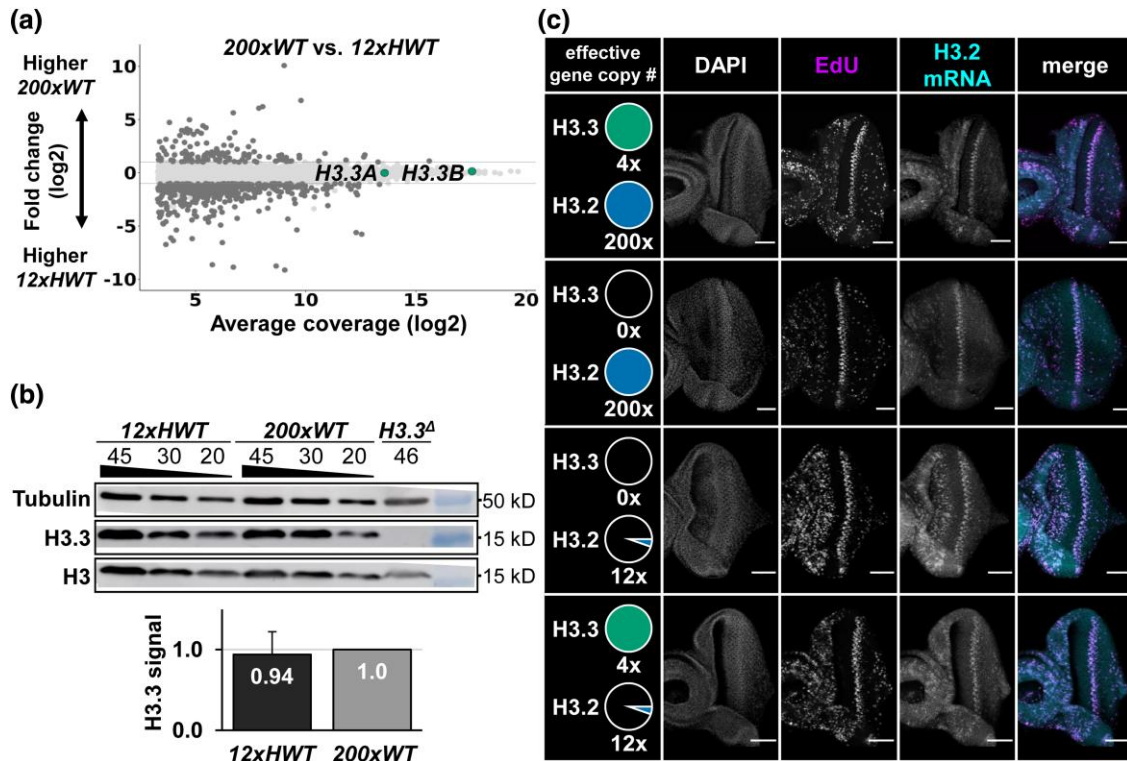
Fig. 2. H3.3 mRNA and protein levels do not change when *H3.2* gene copy number is reduced. a) MA plot showing fold change of normalized third instar larval brain RNA-seq signal in wild-type (*200xWT*) vs *12xHWT* for all transcripts (*y*-axis). Average coverage on the *x*-axis represents the mean expression level of a transcript. Differentially expressed genes are indicated in dark gray. Values for *H3.3A* and *H3.3B* transcripts are indicated (green). b) Western blot of total H3, H3.3, and tubulin from *12xHWT* and *200xWT* wandering third instar larval wing imaginal discs. Dilution series with indicated number of wing discs for each genotype. H3.3$^\Delta$ third instar larvae were used as a negative control. Bar plot depicting the average fold change in H3.3 signal relative to *200xWT* signal normalized to tubulin. Error bars represent standard deviation of three biological replicates. c) Confocal images of third instar imaginal eye discs stained for DAPI (grey), EdU (magenta), and H3.2 mRNA (cyan) for the four indicated genotypes, denoted as in Fig. 1. The maximum projection of four adjacent slices is shown. Bars, 50 μM.

were confirmed by PCR. Primer information can be found in Supplementary Table 11.

RNA sequencing

For each replicate sample, 25 brains were dissected from wandering 3rd instar larvae and homogenized in Trizol solution. RNA was isolated from the Trizol aqueous phase using the Zymo RNA Clean and Concentrator-5 kit (Genesee Scientific #11-352) including treatment with DNAse I, as per the manufacturer's instructions. Libraries were prepared from polyA-selected RNA using the KAPA stranded mRNA kit (Roche # 07962207001) and sequenced using the NOVASeq-S1 paired-end 100 platform. Sequence reads were trimmed for adaptor sequence/low-quality sequence using BBDuk (bbmap v38.67) with parameters: ktrim = *r*, *k* = 23, rcomp = *t*, tbo = *t*, tpe = *t*, hdist = 1, mink = 11. Dm6 genome files for use with the STAR aligner were generated using parameters: sjdbOverhang 99. Paired-end sequencing reads were aligned using STAR v2.7.7a with default parameters (Dobin *et al.* 2013). featureCounts (subread v2.0.1) was used with default parameters to count reads mapping to features (Liao *et al.* 2014). DESeq2 (v1.34.0) was used to identify differentially expressed genes (Love *et al.* 2014). Differentially expressed genes were defined as genes with an adjusted *P*-value less than 0.05 and an absolute log2 fold change greater than 1.

Western blots

Protein extracts from *H3.3^null^* third instar larvae and *12xHWT* and *yw* (*200xWT*) third instar larval wing discs were prepared by boiling samples for 10 minutes in Laemmli SDS-PAGE loading buffer followed by sonication using the Bioruptor Pico sonication system (Diagenode) for 10 cycles (30 sec on, 30 sec off). Samples were clarified by centrifugation. Proteins were fractionated on BioRad Any kD Mini-PROTEAN TGX Precast Protein Gels GX (BioRad #4569033) and were transferred to 0.2 μm nitrocellulose membranes (BioRad #1620112) at 100 V for 10 and 60 V for 20 minutes. Total protein was detected using G-Bioscience Swift Membrane Stain (G-Bioscience, 786677). Membranes were probed using the following antibodies: rabbit anti-H3 (1:60,000; Abcam Cat# ab1791, RRID:AB_302613), rabbit anti-H3.3 (1:1,000, Abcam Cat# ab176840, RRID:AB_2715502), and mouse anti-tubulin (1:15,000, Sigma-Aldrich Cat# T6074, RRID: AB_477582). Western blot analysis was performed using the following HRP conjugated secondary antibodies: goat anti-Mouse-IgG-HRP (1:10,000, Thermo Fisher Scientific Cat# 31430, RRID:AB_228307), donkey anti-Rabbit-IgG-HRP (1:10,000, (Cytiva Cat# NA934, RRID:AB_772206). Blots were detected using Amersham ECL Prime Western blotting Detection Reagent (Cytvia, RPN2232). ImageLab densitometry analysis was used to determine total protein, tubulin, H3.3, and H3 band intensity. Histone signal was normalized to corresponding tubulin signal. Normalized signals from different titrations of the same genotype were averaged and resulting values were set relative to the wild-type value. This process was completed for three biological replicates. See Supplementary Fig. 2 and Supplementary Table 2 for biological replicate blots and signal quantification, respectively.

EdU + RNA-FISH

Third instar larval eye discs were dissected in Grace's medium and incubated in 0.1 mg/mL EdU for 30 minutes. Samples were then washed in phosphate-buffered saline (PBS) for 5 minutes, fixed for 30 minutes in 4% paraformaldehyde (16% paraformaldehyde, diluted in PBS), washed 3× 15 minutes in PBS with Triton (PBST) (0.5% Triton X-100) and washed for 30 minutes in 3% Bovine serum albumin (BSA) in PBS. EdU was detected using the Click-iT EdU Cy5 imaging kit (Invitrogen) according to the manufacturer's instructions. After EdU detection, samples were washed in 3% BSA for 15 minutes, washed in PBS for 5 minutes, and subsequently fixed in 4% paraformaldehyde for 15 minutes. Next, RNA-FISH was performed using Stellaris H3.2 mRNA probes with TAMRA fluorophores following the manufacturer's instructions for *D. melanogaster* wing imaginal discs. Samples were stained with DAPI (1 µg/mL) at 37°C for 30 minutes in Wash Buffer A. The maximum projection from 4 adjacent z-slices from third instar wandering larval eye discs was used as representative images for each genotype. H3.2 RNA-FISH probe set can be found in Supplementary Table 12.

Mitotic recombination

yw; ΔHisC, FRT40A/CyO, twistGFP; 12xHWT males were crossed to *yw, hsFLP; UbiGFP, FRT40A;* females. Adults were removed from the vial after 24 hours. Forty-eight hours later, the vials were heat shocked at 37°C for 8 minutes. *yw, hsFLP/yw; ΔHisC, FRT40A/UbiGFP, FRT40A; 12xHWT/+* third instar wandering larvae were selected based on lack of twistGFP fluorescent signal.

Genetic screen viability

All fly stocks were maintained on standard corn medium at 25°C. Crosses were flipped every other day for 8 days. Progeny were scored once per day. All genotypes and progeny numbers can be found in Supplementary Table 3.

To examine the effect of chromosome 3L mutations on $H3.3^4$; $12xHWT$ viability (Fig. 3b, Fig. 4a):

Bloomington third chromosome deficiency stock males were crossed to *yw; $H3.3A^{2×1}$, ΔHisC, twistGal4/CyO; MKRS/TM6B* virgin females. Subsequently, *yw; $H3.3A^{2×1}$, ΔHisC, twistGal4/+; Df(3)/MKRS* male progeny were crossed with *yw; $H3.3A^{2×1}$, $ΔHisC^{Cadillac}/H3.3A^{2×1}$, $ΔHisC^{Cadillac}$; 12xHWT/12xHWT* virgin females. Animals eclosing from deficiency crosses were counted beginning ten days post egg-laying based on the presence or absence of dsRed from the $ΔHisC^{Cadillac}$ locus and stubble phenotype from MKRS until all adult flies eclosed. Percent of expected was determined by the ratio of *yw; $H3.3A^{2×1}$, ΔHisC, twistGal4/$H3.3A^{2×1}$, $ΔHisC^{Cadillac}$; Df(3)/12xHWT* was to *yw; $H3.3A^{2×1}$, ΔHisC, twistGal4/$H3.3A^{2×1}$, $ΔHisC^{Cadillac}$; MKRS/12xHWT* siblings. Significance was determined by a Chi-square test. Observed value is the number of *yw; $H3.3A^{2×1}$, ΔHisC, twistGal4/$H3.3A^{2×1}$, $ΔHisC^{Cadillac}$; Df(3)/12xHWT* progeny and expected value is the number of *yw; $H3.3A^{2×1}$, ΔHisC, twistGal4/$H3.3A^{2×1}$, $ΔHisC^{Cadillac}$; MKRS/12xHWT* progeny. Thresholds of $P < 0.05$ and $P < 0.01$ were used in this study.

To examine the effect of Pc^3 on $H3.3^4$ viability (Fig. 6a):

$H3.3B^0/H3.3B^0$; $H3.3A^{2×1}/CyO$, twistGFP; x yw; $H3.3A^{2×1}/CyO$; Pc^3/MKRS. Animals eclosing were counted beginning ten days post egg-laying based on the presence or absence of curly wings from CyO and stubble phenotype from MKRS until all adult flies eclosed. Percent of expected was determined by the ratio of *$H3.3B^0/Y$; $H3.3A^{2×1}/H3.3A^{2×1}$; Pc^3/ +* to *$H3.3B^0/Y$; $H3.3A^{2×1}/H3.3A^{2×1}$; MKRS/ +* siblings. Significance was determined by a Chi-square test. Observed value is the number of *$H3.3B^0/Y$;*

$H3.3A^{2×1}/H3.3A^{2×1}$; Pc^3/ + progeny and expected value is the number of *$H3.3B^0/Y$; $H3.3A^{2×1}/H3.3A^{2×1}$; MKRS/ +* progeny. Thresholds of $P < 0.05$ and $P < 0.01$ were used in this study.

To examine the effect of Pc^3 on $12xHWT$ viability (Fig. 6a):

Yw/Y; ΔHisC, twistGal4/CyO; Pc^3/TM6B x yw; ΔHisC, UAS-YFP/CyO; 12xHWT/12xHWT. Animals eclosing were counted beginning ten days post egg-laying based on the presence or absence of curly wings from CyO and humoral phenotype from TM6B until all adult flies eclosed. Percent of expected was determined by the ratio of *yw; ΔHisC, twistGal4/ΔHisC, UAS-YFP; Pc^3/12xHWT* to *yw; ΔHisC, twistGal4/ΔHisC, UAS-YFP; TM6B/12xHWT* siblings. Significance was determined by a Chi-square test. Observed value is the number of *yw; ΔHisC, twistGal4/ΔHisC, UAS-YFP; Pc^3/12xHWT* progeny and expected value is the number of *yw; ΔHisC, twistGal4/ΔHisC, UAS-YFP; TM6B/12xHWT* progeny. Thresholds of $P < 0.05$ and $P < 0.01$ were used in this study.

Immunofluorescence

For Ubx and H3.3 staining of wing discs, third instar larval cuticles were inverted and fixed in 4% paraformaldehyde in PBS for 20 minutes at room temperature. Cuticles were washed for 1 h in PBST (0.15% Triton X-100). Mouse anti-UBX (1:30, DSHB Cat# FP3.38, RRID:AB_10805300) and mouse anti-H3.3 (1:500, Abnova Cat# H00003021-M01, RRID:AB_425473) were used overnight at 4°C. Goat anti-mouse IgG secondary antibody (1:1000, Thermo Fisher Scientific Cat# A-11029, lot #161153, RRID:AB_2534088) was used for 2 hours at room temperature. DNA was counterstained with DAPI (0.2 µg/mL) and the discs were mounted in Vectashield (VWR, 101098-042) mounting media and imaged on a Leica Confocal SP8.

Scanning electron microscopy

One- to four-day-old flies were dehydrated in ethanol and images of legs were taken using a Hitachi TM4000Plus tabletop SEM microscope at 15 kV and 500× magnification.

Results
H3.3 is required for viability when *H3.2* gene copy number is reduced

To examine whether coordination between canonical *H3.2* and variant *H3.3* gene expression contributes to *Drosophila* development, we measured the effects of altering the relative number of canonical vs variant histone gene copies on viability and fertility. Zygotes lacking all canonical histone genes (*ΔHisC*) arrest early in embryonic development, and this lethality can be rescued with a transgene encoding 12 tandemly arrayed histone gene repeats (*12xHWT*), providing an opportunity to manipulate canonical histone gene dose over an ~18-fold range (Fig. 1, a and d) (McKay *et al.* 2015). Null mutations of either *H3.3A* or *H3.3B* have no effect on viability or fertility of flies containing the normal complement of canonical histone genes (Supplementary Table 1), but only 50% of the expected number of *H3.3A, H3.3B* double mutants (*$H3.3^4$; 200xWT*) eclose as adult flies, which are infertile (Fig. 1d) (Sakai *et al.* 2009). *$H3.3^4$* animals heterozygous for a *HisC* deletion (*$H3.3^4$; 100xWT*) survive to adulthood at a similar frequency as *$H3.3^4$; 200xWT* animals (54.2 and 50% of expected, respectively) (Fig. 1d). However, reducing canonical histone gene copy number to 20 (*$H3.3^4$; 20xHWT*) results in only 17.1% of the expected number of adults (Fig. 1d). A further reduction to 12 histone gene repeats (*$H3.3^4$; 12xHWT*) results in a complete loss of viability of flies lacking variant *H3.3* genes (Fig. 1d). *$H3.3^4$; 12xHWT* lethality is rescued by one copy of either *H3.3A* or *H3.3B*, and the adults
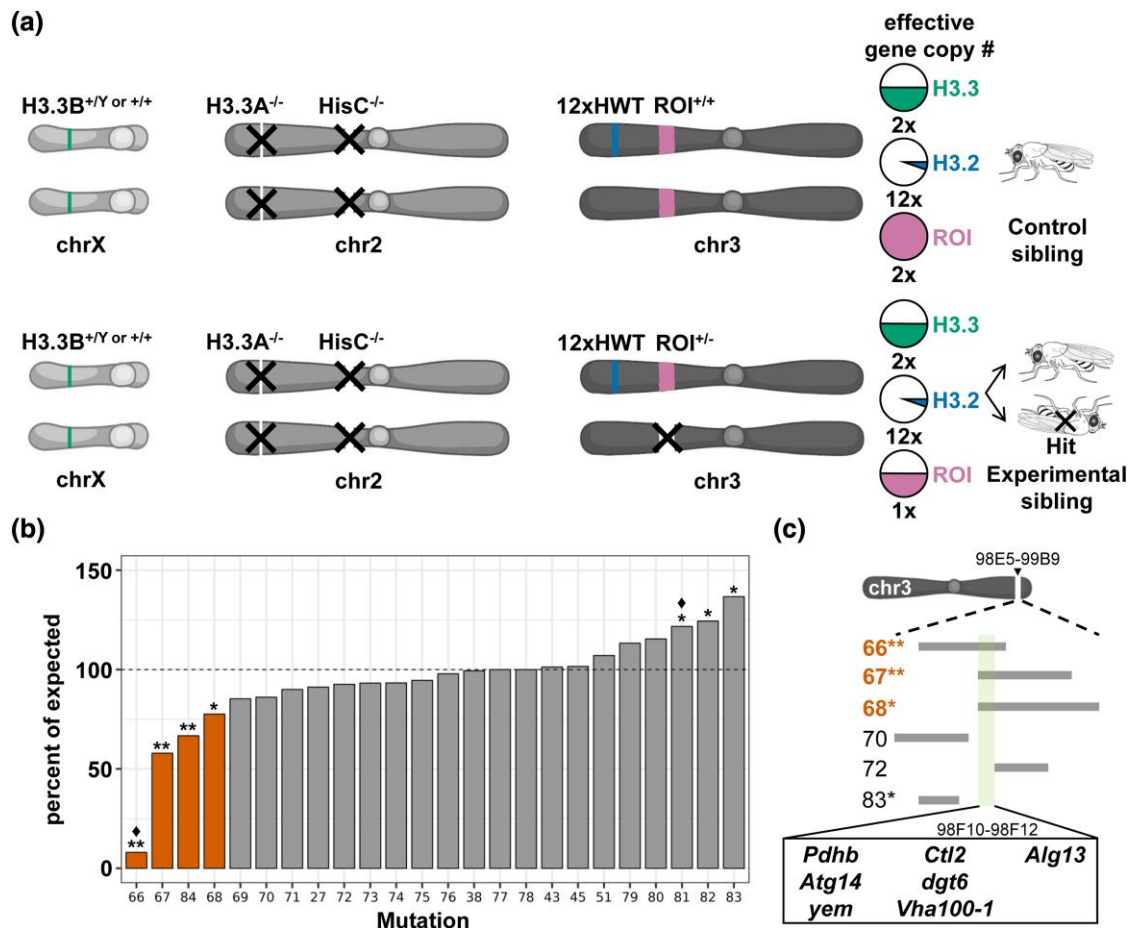
Fig. 3. A genetic screen to identify genes required for survival when *H3* gene copy is reduced. a) Schematic of the screen used to identify regions of interest (ROI) on chromosome 3 that when heterozygous or hemizygous reduce adult viability of the *H3.3A^A; 12xHWT* experimental genotype compared to control siblings. H3 gene copy number indicated as in Fig. 1. Pink fill indicates gene copy number of the ROI. b) Bar plot of viability for 23 mutations on chr3L and chr3R (see Table 1). Asterisks indicate statistical significance by Chi-square test (** $P < 0.01$, * $P < 0.05$, ♦ potential haploinsufficiency irrespective of *H3* gene copy number, see Supplementary Table 3 for *P*-values). Deficiencies covering region of interest indicated by orange bars. Data are plotted as the percent of *H3.3A^A; 12xHWT* animals inheriting the deficiency chromosome relative to sibling animals inheriting the homologous balancer chromosome, which establish the expected percentage (dashed line). c) Diagram of deficiencies that delineate a region of interest on chr3R from 98E5-99B9. The overlapping region specific to the positive hits from 98F10-98F12 contains seven genes (green bar).

of these genotypes are fertile (Fig. 1d and Supplementary Table 1). Thus, we conclude that *H3.3* expression is necessary for completion of development when canonical histone gene copy number is reduced to 12, and that the probability of animals lacking *H3.3* to complete development increases with increasing numbers of canonical histone genes. Furthermore, our data support previous observations that *H3.3* is required for male and female fertility (Fig. 1d) (Sakai *et al.* 2009). Collectively, these data suggest that *H3.3* compensates for reduced *H3.2* gene copy number to maintain a critical threshold of total H3 protein.

H3.3 mRNA and protein levels do not change when H3.2 gene copy number is reduced

Mechanisms that compensate for altered variant vs canonical histone genes could operate at many levels, including transcription, translation, histone deposition into chromatin, or histone protein turnover. For instance, increased *H3.3* expression could compensate for reduced *H3.2* gene copy number, potentially explaining why *12xHWT* animals do not survive in the absence of *H3.3* genes. We reasoned that measuring steady-state mRNA and protein levels could reveal evidence of such compensatory mechanisms. To determine whether *H3.3* steady-state mRNA levels are elevated

in *12xHWT* animals, we compared *H3.3* mRNA levels in *12xHWT* vs *200xWT* control animals in an RNA-sequencing data set obtained from third instar larval brains. We found no significant difference in *H3.3A* or *H3.3B* mRNA levels in *12xHWT* compared to *200xWT* cells (Fig. 2a). Consistent with these RNA-seq data, immunoblots of third instar larval wing imaginal discs show comparable levels of H3.3 protein in *12xHWT* and *200xWT* controls (Fig. 2b). Moreover, immunofluorescence of genetically mosaic third instar larval wing discs generated by mitotic recombination show similar levels of H3.3 protein in clones of *12xHWT* cells and *212xHWT* control cells (Supplementary Fig. 1). We conclude that compensation for reduced *H3.2* gene copy number in *12xHWT* animals does not occur via detectable changes in the steady-state levels of *H3.3* mRNA or protein, as measured by RNA-sequencing, immunoblotting, or immunofluorescence.

We considered the possibility that expression of *H3.2* becomes uncoupled from S phase upon loss of *H3.3*, thereby maintaining a pool of H3 outside of S phase even when *H3.3* genes are absent. To determine whether *H3.2* transcripts are present in cells outside of S phase in the absence of *H3.3* genes, we combined EdU staining with RNA-fluorescent *in situ* hybridization (FISH) in the developing eye of *200xWT*, *H3.3^A*, *H3.3^A; 12xHWT,* and *12xHWT* animals. We
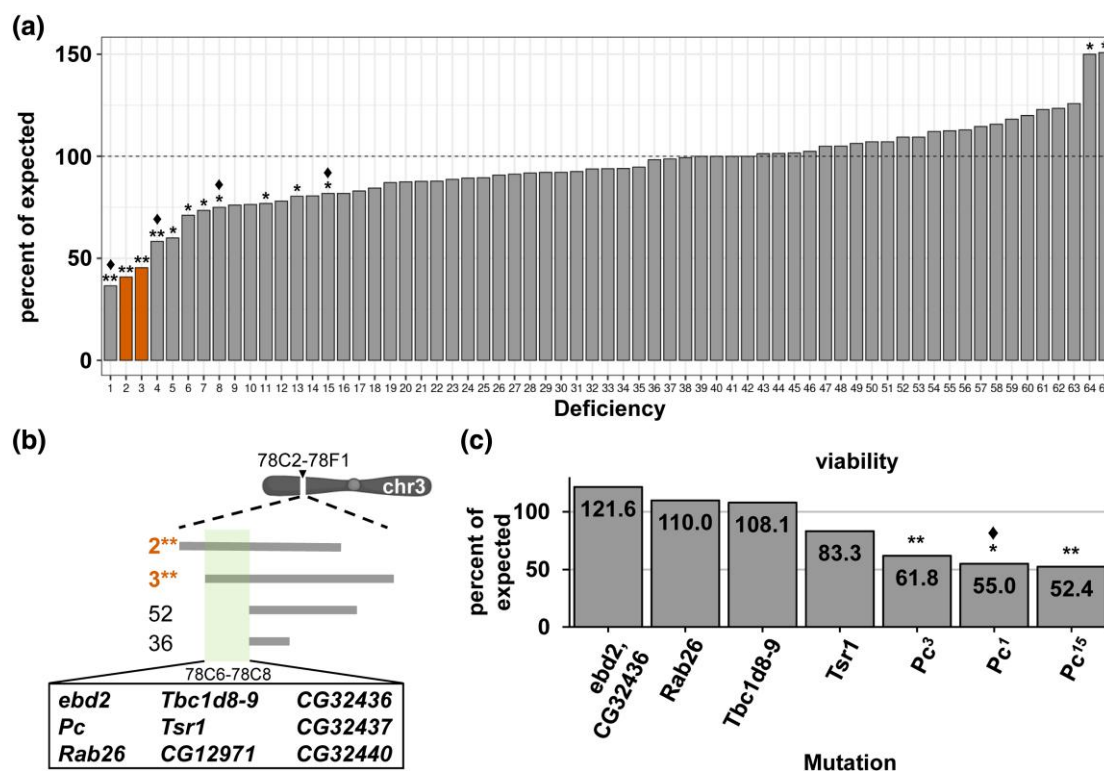
Fig. 4. Screen of chromosome 3L deficiencies identifies a genetic interaction between *Polycomb* and histone *H3* gene copy number. a) Bar plot of viability for 65 chr3L deficiency mutations (see Table 2). Orange bars indicate two overlapping deficiencies that scored positive and uncover the *Pc* locus. Data are plotted as in Fig. 3. b) Diagram of deficiencies that delineate a region of interest on chr3L from 78C2–78F1. The overlapping region specific to the positive hits from 78C6–78C8 contains nine genes (green bar). *Df(3L)BSC435* (*Df* 2) and *Df(3L)BSC419* (*Df* 3) correspond to the orange bars in panel A. c) Bar plot of viability of *H3.3A⁴; 12xHWT* animals heterozygous for the seven indicated mutations. Data are plotted as in Fig. 3. Asterisks indicate statistical significance by Chi-square test (** P value < 0.01, * P value < 0.05, ♦ potential haploinsufficiency irrespective of *H3* gene copy number, see Supplementary Table 3 for *P*-values).

observed that *H3.2* mRNA is only detected in EdU-positive cells in all four genotypes, indicating that *H3.2* transcription is not uncoupled from S phase when *H3.2* and/or *H3.3* gene copy number are reduced (Fig. 2c). In addition, we observed via FISH that the levels of *H3.2* mRNA are similar in *12xHWT* cells compared to *200xWT* controls. Similar findings were reported previously in early *D. melanogaster* embryos via RT-PCR, suggesting a mechanism of histone dosage compensation at the transcriptional level (McKay *et al.* 2015).

A genetic screen for genes sensitive to reduced histone H3 gene copy number

The inability to detect evidence of histone gene coordination at the molecular level motivated us to instead take an unbiased genetic approach. Performing a screen in a genotype with reduced variant and canonical histone gene copy number could potentially identify genes that: (1) regulate histone gene expression, (2) coordinate expression between variant and canonical histone genes, or (3) are otherwise sensitive to reduced histone levels. As described above, *12xHWT* animals are viable and fertile at wild-type frequencies (Fig. 1d); however, *H3.3⁴; 12xHWT* flies are inviable (Fig. 1d). We therefore reasoned that we could identify other genes that when mutated would reduce the viability of *12xHWT* animals. Because having one copy of *H3.3A* or *H3.3B* is sufficient to retain viability in a *12xHWT* background (Fig. 1d), we decided to screen using a *12xHWT* background that is further sensitized by the removal of both copies of *H3.3A*. We refer to this genotype as *H3.3A⁴; 12xHWT* (Fig. 3a).

First, we conducted a proof-of-principle screen using single gene loss of function alleles or deficiencies covering genes with potential roles in histone function. We tested histone H3 chaperones (e.g. *Asf1*, *Yem*, *Xnp*), cell cycle regulators (e.g. *E2F*, *Stg*), and genes involved in the control of histone mRNA synthesis or chromatin regulation (e.g. *Slbp*, *wge*, *Arts*, *Dre4*). We performed crosses that produced *H3.3A⁴; 12xHWT* progeny heterozygous for individual mutations or deficiencies and determined whether the progeny had reduced or increased viability compared to *H3.3A⁴; 12xHWT* control siblings. Of the 23 mutations tested, heterozygosity of three deficiency mutations—*Df(3R)BSC874* (*Df* 66), *Df(3R)BSC500* (*Df* 67), and *Df(3R)BSC501* (*Df* 68)—resulted in a significant reduction in viability of *H3.3A⁴; 12xHWT* flies compared to control siblings, with only 8.4%, 57.9%, and 77.6% of expected surviving to adulthood, respectively (Fig. 3b, orange bar and Table 1). Interestingly, three other deficiencies *Df(3R)ro80b* (*Df* 81), *Df(3R)BSC527* (*Df* 82), and *Df(3R)Exel6210* (*Df* 83) resulted in a significant increase in viability of *H3.3A⁴; 12xHWT* flies compared to control siblings, but we did not pursue these further (Fig. 3b and Table 1). Heterozygosity of the region covered by *Df* 81 results in an increase in viability independent of histone gene copy number (Fig. 3b, diamond). Notably, the three deficiencies (*Df* 66, *Df* 67, and *Df* 68) that reduce *H3.3A⁴; 12xHWT* viability overlap the same 79.1 kb region on chromosome 3R (Fig. 3c). To further define the genomic interval responsible for the genetic interaction, we tested three additional deficiencies that partially overlap this region. *Df(3R)BSC789* (*Df* 70), *Df(3R)ED6310* (*Df* 72), and *Df* 83 did not result in a significant reduction in viability. Therefore, the region of
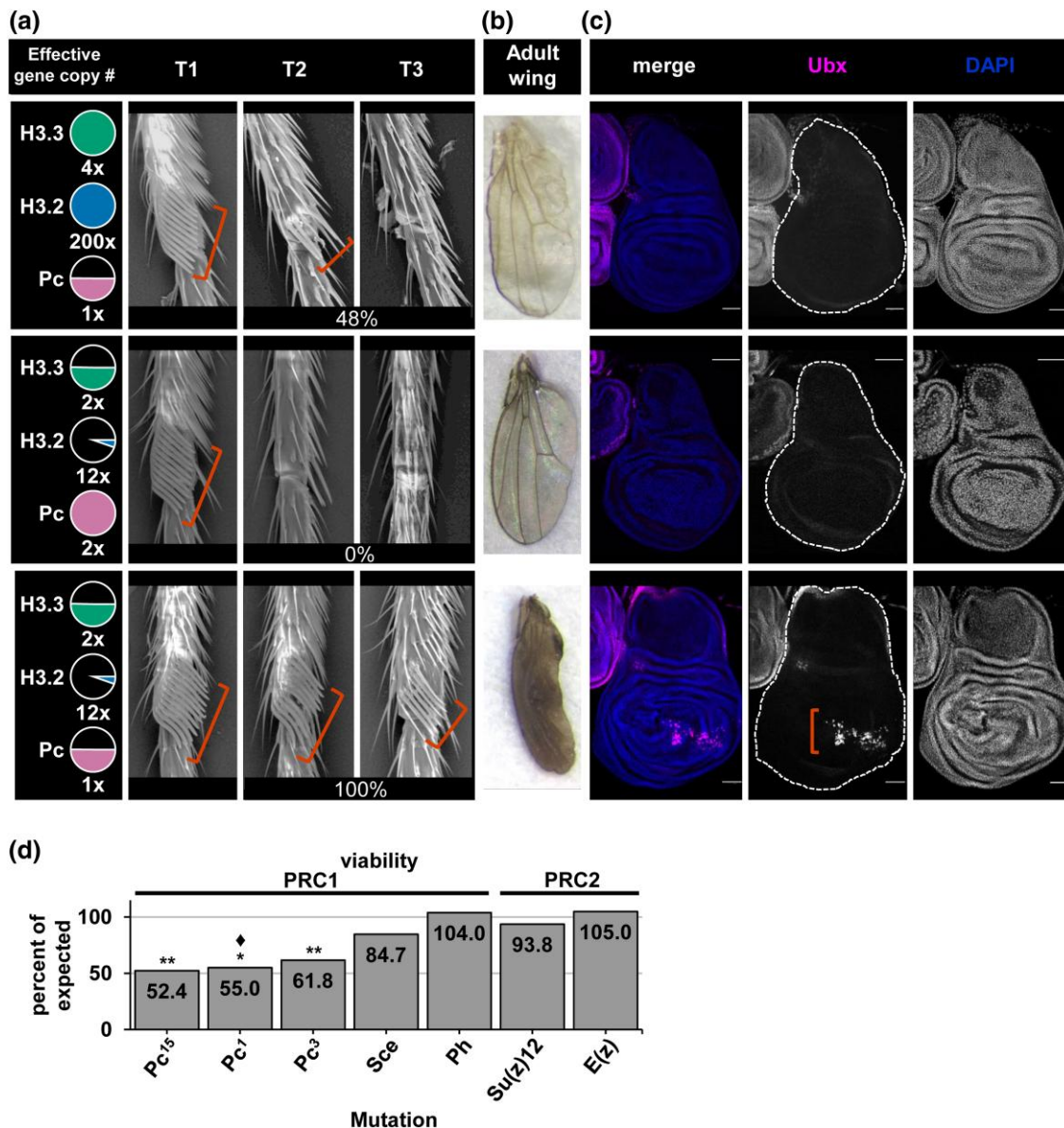
Fig. 5. Reduced histone *H3* gene copy number disrupts Polycomb-mediated gene repression. a) Scanning electron micrographs of first (T1), second (T2), and third (T3) thoracic legs from adult males of the indicated genotypes, depicted as in Fig. 1 with *Pc* gene dose in pink. Red brackets indicate the location where sex combs developed. Percent of T2 and T3 legs with ectopic sex combs indicated for each genotype. b) Bright field images of adult wings from the indicated genotypes. c) Confocal images of wing imaginal discs of the indicated genotypes stained for DAPI (blue) and Ubx (magenta). Red brackets indicate the wing pouch where ectopic Ubx expression occurred. Bars, 50 µM. d) Bar plots of viability of *H3.3A^4; 12xHWT* animals heterozygous for mutations of PRC1 and PRC2 Polycomb complex members. Data are plotted as in Fig. 3. Asterisks indicate statistical significance by Chi-square test (** P < 0.01, ◆ potential haploinsufficiency irrespective of *H3* gene copy number, see Supplementary Table 3 for P-values). *Pc^3* was used in panels A and B. *Pc^15* was used in panel C.

interest is limited to a 26.4 kb region defined by the left breakpoints of *Df 67* and *Df 72* at genomic positions 98F10 and 98F12 (Fig. 3c). Seven annotated genes reside within this region of interest: *Alg13*, *Atg14*, *Ctl2*, *dgt6*, *Pdhb*, *Vha100-1*, and *yem* (Fig. 3c). Because Yem is an H3.3 specific chaperone, we next tested heterozygosity of a *yem* amorphic allele, which resulted in a significant reduction in viability, with only 66.7% of expected surviving to adulthood (Fig. 3b and Supplementary Table 3). One possible explanation for these genetic results is that heterozygosity of *yem* attenuates incorporation of H3.3 protein (derived from the *H3.3B* locus) into chromatin enough to reduce the viability of *H3.3A^4; 12xHWT* flies. This targeted screen confirms that our genetic paradigm can identify mutant loci that when hemizygous cause sensitivity to a reduction in H3.2 and H3.3 gene copy number.

To expand our search for such loci, we screened the left arm of chromosome 3 (chr3L) using the Bloomington Stock Center Chr3L Deficiency Kit (Supplementary Table 8), which consists of 77 stocks that cover 97.1% of the chr3L euchromatic genome (Cook *et al.* 2012; Roote and Russell 2012). Fourteen of the deficiency mutations were excluded from the screen because they carry a mini-white genetic marker, resulting in an eye color that precludes identifying all progeny classes (Supplementary Table 8). Of the 60 deficiency mutations screened, two resulted in an increase in viability when heterozygous in *H3.3A^4; 12xHWT* flies (Fig. 4a, asterisks and Table 2), which we did not pursue further. By contrast, heterozygosity of eleven deficiencies caused significant reductions in viability of *H3.3A^4; 12xHWT* flies (Fig. 4a, asterisks and Table 2). Four of these deficiencies (*Df 1*, *Df 4*, *Df 8*, and *Df 15*)
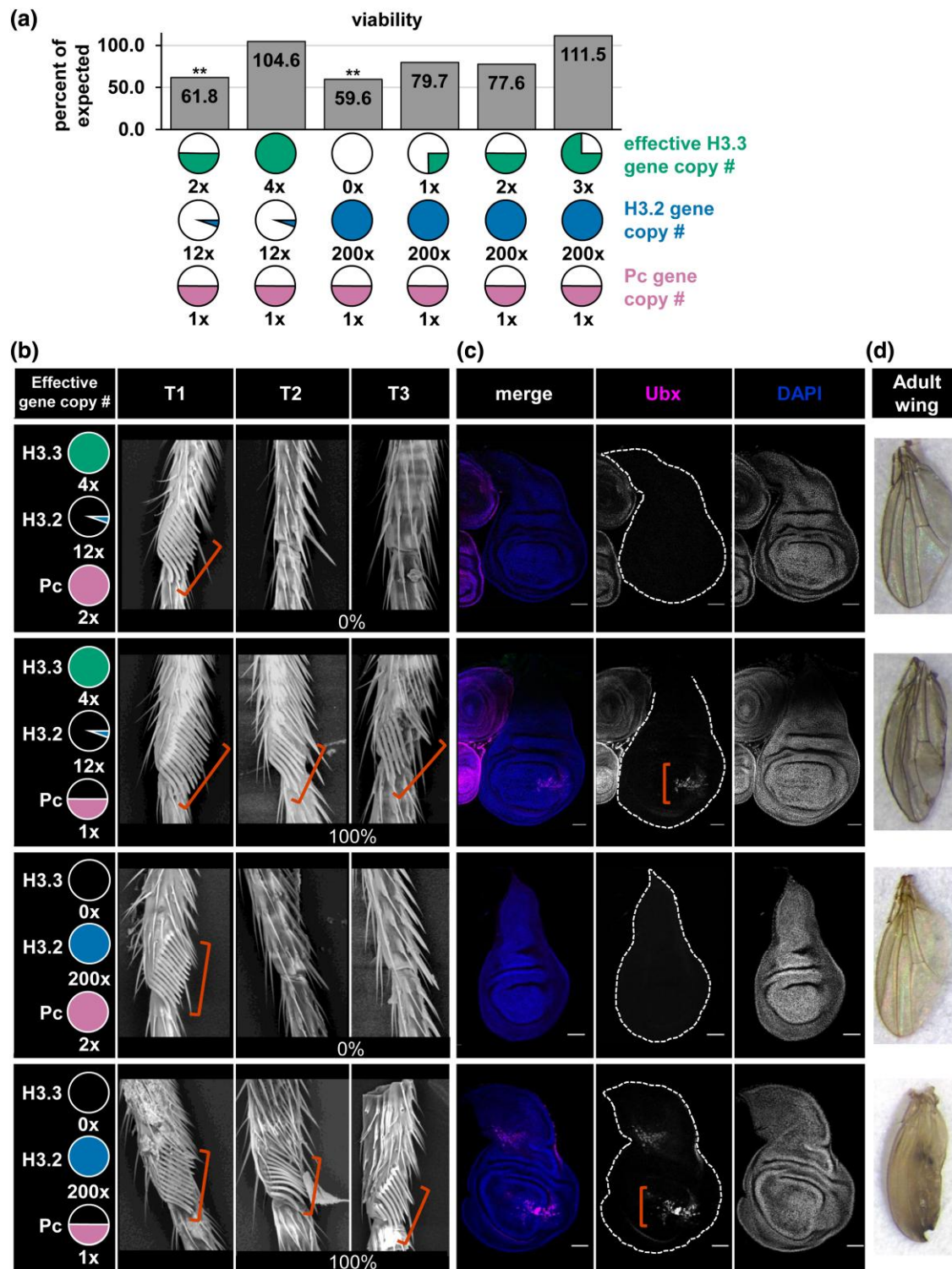
Fig. 6. Polycomb-mediated gene repression is sensitive to both *H3.2* and *H3.3* gene copy number. a) Bar plot of viability for the indicated genotypes, depicted as in Fig. 1 with *Pc* gene dose in pink. Data are plotted as in Fig. 3. Asterisks indicate statistical significance by Chi-square test (** *P* < 0.01, see Supplementary Table 6 for *P*-values). b) Scanning electron micrographs of first (T1), second (T2), and third (T3) thoracic legs from adult males of the indicated genotypes. Red brackets indicate the location where sex combs developed. Percent of T2 and T3 legs with ectopic sex combs indicated for each genotype. c) Confocal images of wing imaginal discs of the indicated genotypes stained for DAPI (blue) and Ubx (magenta). Red brackets indicate the wing pouch where ectopic Ubx expression occurred. Bars, 50 μM. d) Bright field images of adult wings of the indicated genotypes. *Pc*[3] was used in panels B and D. *Pc*[15] was used in panel C.

also caused a significant reduction in viability of siblings with one copy of *H3.3A*, one copy of *HisC* (100x), and the *12xHWT* transgene (*H3.3A*[+/-]; *112xHWT*), suggesting haploinsufficiency (Fig. 4a, diamonds). We did not pursue these hits further. Interestingly, of

the remaining hits *Df(3L)BSC435* (*Df 2*) and *Df(3L)BSC419* (*Df 3*) overlap the same 293 kb region of chr3L (Fig. 4b, orange). To map the genetic interaction in greater detail, we obtained two additional deficiencies—*Df(3L)BSC418* (*Df 52*) and *Df(3L)BSC836*

Table 1. Chromosome 3R and 3L mutation alleles tested in proof-of-principle screen for changes in viability.

Number[a]	Deficiency	Start coordinate[b]	End coordinate[b]	P value[c]
27	*Df(3L)BSC289*	1332329	1628100	-
45	*Df(3L)ED4287*	1795442	2551761	-
79	*Df(3L)ED4284*	1795442	1963552	-
80	*Df(3L)BSC385*	2259731	2417382	-
38	*Df(3L)BSC730*	12156077	12836424	-
51	*Df(3L)ED4606*	16080584	16773223	-
43	*Df(3L)BSC220*	18965662	19164368	-
77	*Asf1[1]*	19619559	19619559	-
78	*E2F[rM729]*	21626545	21626545	-
82	*Df(3R)BSC527*	22626930	23111808	+
71	*Df(3R)ED6220*	24543798	25183773	-
73	*Df(3R)10-65*	81F	81F	-
76	*Df(3R)XNP[1]*	25477868	25482834	-
81◆	*Df(3R)ro80b*	97D1	97D13	+
75	*Df(3R)BSC460*	27937830	28461658	-
83	*Df(3R)Exel6210*	28674961	28991018	+
66◆	*Df(3R)BSC874*	28675029	29191671	++
70	*Df(3R)BSC789*	28820134	29040507	-
67	*Df(3R)BSC500*	29112527	29675700	++
68	*Df(3R)BSC501*	29112527	29724685	+
84	*Yem[2]*	29119694	29122874	++
72	*Df(3R)ED6310*	29138895	29512153	-
74	*Stg[4]*	29252826	29255800	-
69	*Df(3R)BSC547*	29621303	29821399	-

[a] ◆ suggested haploinsufficiency.
[b] Breakpoints are as determined by the Bloomington stock center.
[c] +, $P < 0.05$; ++, $P < 0.01$. P-values obtained from a Chi-square test. See Supplementary Table 4 for P-values.

(*Df* 36)—that overlap this same region of chr3L and observed no changes in viability of *H3.3A[A]; 12xHWT* flies compared to control siblings (Fig. 4, a and b). Therefore, the genomic region spanning 77.8 kb on chr3L between cytological positions 78C6 and 78C8 impairs viability of flies with reduced *H3.3* and *H3* gene copy number.

Reduced histone *H3* gene copy number disrupts Polycomb-mediated gene repression

Nine annotated genes reside within the defined genomic interval: *CG12971, CG32436, CG32437, CG32440, ebd2, Pc, Rab26, Tbc1d8-9,* and *Tsr1* (Fig. 4b). To determine which of these genes contributes to viability of flies with reduced histone gene copy number, we generated *H3.3A[A]; 12xHWT* animals heterozygous for single gene mutations. *CG12971, CG32437,* and *CG32440* were not tested because no loss-of-function alleles exist. Heterozygous MiMIC transposon insertion alleles of *ebd2, Rab26, Tbc1d8-9, Tsr1,* and *CG32436* did not impact viability of *H3.3A[A]; 12xHWT* flies (Fig. 4c). However, three independent alleles of the *Polycomb* gene—*Pc[1], Pc[3],* and *Pc[15]*—resulted in significant reductions in viability of *H3.3A[A]; 12xHWT* flies (55.0, 61.8, and 52.4% of expected survive to adulthood, respectively) (Fig. 4c). These data suggest that *H3.3A[A]; 12xHWT* flies are less viable when Polycomb function is reduced.

Polycomb group genes encode evolutionarily conserved regulators of cell identity. Polycomb complexes function to heritably silence expression of master regulator genes, including the Hox genes, which specify segmental identity (Kassis *et al.* 2017). In adult males, reduction of Polycomb function can result in homeotic transformations whereby the second (T2) and third (T3) thoracic legs acquire morphological features normally found only on the first thoracic legs (T1). This is most notably manifest by the appearance of sex combs on T2 and T3 legs, which normally only occur on T1 legs (Kaufman *et al.* 1980; Pattatucci *et al.* 1991). Based on

our identification of the *Pc* gene in our genetic screen, we hypothesized that reduced histone gene copy number compromises Polycomb complex function. A prediction of this hypothesis is that reduced histone gene copy number would enhance *Pc* mutant phenotypes. Therefore, we evaluated the frequency and severity of homeotic transformations in *H3.3A[A]; 12xHWT* animals heterozygous for a *Pc* null mutation (*H3.3A[A]; 12xHWT; Pc[3/+]*). We observed that *H3.3A[A]; 12xHWT; Pc[3/+]* males exhibit an increased frequency of ectopic sex combs (100%, Fig. 5a, row 3) on T2 and T3 legs relative to *Pc[3/+]* (48%, Fig. 5a, row 1) or *H3.3A[A]; 12xHWT* males (0%, Fig. 5a, row 2) (Table 3). Moreover, the expressivity of the ectopic sex comb phenotype is more severe in *H3.3A[A]; 12xHWT; Pc[3/+]* animals relative to *Pc[3/+]* controls, often having a full set of sex combs on T2 and T3 legs (Fig. 5a, rows 1 and 3). Males and females of this genotype also exhibit defects in posterior wing morphology (Fig. 5b, row 3), suggesting partial wing to haltere transformation due to a failure to maintain proper repression of *Ubx* in the wing. Consistent with this hypothesis, immunostaining of *H3.3A[A]; 12xHWT; Pc[15/+]* third instar imaginal wing discs revealed ectopic *Ubx* expression in the pouch region (Fig. 5c, row 3). We conclude that histone *H3* gene copy number contributes to Polycomb function during development.

Next, we determined whether mutations in other Polycomb group genes cause effects similar to mutations of *Pc* when histone *H3* gene copy number is reduced. *H3.3A[A]; 12xHWT* flies heterozygous for null mutations in *Sce* and *Ph*, which encode members of Polycomb Repressive Complex 1 (PRC1), are viable at expected frequencies (Fig. 5d). Similarly, heterozygous mutations in Polycomb Repressive Complex 2 (PRC2) genes, *E(z)* and *Su(z)12*, do not cause reductions in viability (Fig. 5d). Moreover, RNA-seq revealed that no Polycomb group genes are differentially expressed in *12xHWT* larval brains compared to control (Supplementary Table 10). Unlike other members of PRC1, Pc directly interacts with histones trimethylated at lysine 27 which may make it uniquely sensitive to histone *H3.2* and *H3.3* gene copy number.

Histone *H3.2* and *H3.3* gene copy number are each critical for Polycomb-mediated gene repression

Since both *H3.2* and *H3.3* gene copy number are reduced in *H3.3A[A]; 12xHWT* animals, we next determined the individual requirement of either *H3.2* or *H3.3* gene copy number in Polycomb-mediated gene repression. We quantified viability and assessed whether Polycomb target genes were de-repressed in either *12xHWT* or *H3.3[A]* animals that were also heterozygous for a *Pc* null mutation (*12xHWT; Pc[3/+]* and *H3.3[A]; Pc[3/+]*, respectively). *12xHWT; Pc[3/+]* animals are viable at expected frequencies (Fig. 6a) but have an increased frequency of ectopic sex combs on T2 and T3 legs like *H3.3A[A]; 12xHWT; Pc[3/+]* animals (Fig. 6b, row 2 and Table 3). *12xHWT; Pc[3/+]* animals also exhibit ectopic *Ubx* expression in the wing pouch of third instar imaginal discs and defects in adult posterior wing morphology (Fig. 6, c and d, row 2). *112xHWT; Pc[3/+]* animals are viable at the expected frequency (Supplementary Table 6) but also exhibit increased frequencies of ectopic sex combs on T2 and T3 legs relative to *Pc[3/+]* controls (Table 3). Of note, the frequency of ectopic sex combs in *112xHWT; Pc[3/+]* animals (80%) is significantly lower than *12xHWT; Pc[3/+]* animals (100%) (Table 3). Thus, reducing *H3.2* gene dose makes animals sensitive to reduced Polycomb function, and the severity of homeotic transformation is proportional to canonical histone gene copy number. We also found that normal *H3.3* gene dose is necessary for Polycomb function. *H3.3[A]; Pc[3/+]* animals are not fully viable, with only 59.6% of expected surviving to adulthood (Fig. 6a). *H3.3[A]; Pc[3/+]* males also exhibit increased frequencies of ectopic

sex combs on T2 and T3 legs (100%, Fig. 6b, row 4 and Table 3), *Ubx* de-repression in the wing pouch of third instar imaginal wing discs (Fig. 6c, row 4), and defects in adult posterior wing morphology (Fig. 6d, row 4). Animals with one or two copies of *H3.3* survive to adulthood at a similar frequency—79.7 and 77.6% of expected, respectively—and animals with three copies of *H3.3* are viable at the expected frequency (Fig. 6a). Consistent with these observations, males with only one copy of *H3.3B* also exhibit ectopic sex combs on T2 and T3 legs (Table 3). Taken together, these findings indicate that both *H3.2* and *H3.3* gene copy number are independently important for Polycomb-mediated gene repression, but viability is only affected by reduction in *H3.3* gene copy number.

Discussion

In this study, we found that reducing either canonical or variant histone *H3* gene copy number disrupts Polycomb-mediated gene repression. Two major protein complexes establish and maintain Polycomb-mediated repression: PRC1 and PRC2. PRC2 catalyzes H3K27me3, both PRC2 and PRC1 bind to H3K27me3, and PRC1 facilitates repression of local chromatin (Blackledge and Klose 2021). Mutations in core components of PRC1 and PRC2 disrupt the formation of these domains and cause transcriptional de-repression of Polycomb targets, such as Hox genes (Kennison and Tamkun 1988; Paro 1990; Orlando 2003). We found that reduction in canonical or variant *H3* gene copy number results in homeotic transformations associated with de-repression of the Polycomb target genes *Ubx* (posterior wing transformation) and *Scr* (ectopic sex comb development in males). Consistent with these findings, a previous study in *D. melanogaster* found that heterozygosity of *HisC* suppresses homeotic transformation phenotypes in animals with a mutation that causes ectopic silencing of Polycomb target genes (Bajusz *et al.* 2001). Reduction of canonical histone gene copy number in *D. melanogaster* also modifies position-effect variegation, a phenomenon mediated by H3K9me3-marked constitutive heterochromatin (Moore *et al.* 1979; Moore *et al.* 1983; Sinclair *et al.* 1983). Moreover, deletion of all variant *H3.3* gene copies in mouse embryonic fibroblasts results in disruption of heterochromatin domains at pericentromeric repeat regions, centromeres, and telomeres (Jang *et al.* 2015). Collectively, these findings indicate that *H3.2* and *H3.3* gene copy number play an important role in establishing efficient silencing via H3K9me3- and H3K27me3-mediated heterochromatin. We discuss below potential mechanisms for how changes in histone gene copy number might impact Polycomb-mediated repressive chromatin.

Histone protein abundance and stoichiometry may influence Polycomb-mediated repressive chromatin

Here, we show that although *12xHWT* animals develop normally, reducing *Pc* gene dose by half in a *12xHWT* background results in mutant phenotypes associated with impaired Polycomb-mediated gene repression. This genetic interaction suggests that the combination of reduced amounts of canonical histones and Polycomb prevents the proper formation of a repressive chromatin domain at Polycomb-silenced genes. However, our previous work found that canonical histone transcript levels are similar in *12xHWT* and *200xWT* animals, at least in early embryos (11), and here we found similar levels of total H3.3 and H3 protein in *12xHWT* and *200xWT* animals by western blotting. H3.2 and H3.3 are highly abundant proteins, and western blots may not provide the sensitivity needed to identify small changes in H3 protein levels that

could be biologically meaningful. Moreover, a subtle decrease in histone protein abundance may result in changes in nucleosome occupancy that preferentially affect heterochromatin function. Polycomb chromatin domains have elevated nucleosome occupancy and decreased nucleosomal spacing and therefore may be particularly sensitive to changes in histone abundance (King *et al.* 2018). In fact, disruption of PRC1-mediated chromatin compaction in *D. melanogaster* results in de-repression of Hox genes (Bonnet *et al.* 2022). In addition to direct effects of decreased histone abundance at Polycomb target genes, it is also possible that indirect effects contribute to Polycomb target gene misregulation in *12xHWT* animals. Previous work showed that reductions in the concentration of free histone H3 results in increased local histone recycling during replication in *Xenopus* egg extracts and *D. melanogaster* embryogenesis (Gruszka *et al.* 2020; Mühlen *et al.* 2023). Thus, another possibility is that reduced histone gene copy number results in an increased proportion of recycled histones within chromatin. If recycled histones carry PTMs that antagonize Polycomb function, such as H3K36me3, they could alter the PTM landscape and impact target gene repression at Polycomb domains (Finogenova *et al.* 2020; Bonnet *et al.* 2022; Mühlen *et al.* 2023; Salzler *et al.* 2023). Future studies examining chromatin accessibility and the PTM landscape at Polycomb target domains upon reduction in *H3* gene copy number would help address these issues.

Nucleosomes and histone-chaperone complexes are multiprotein complexes that assemble with defined stoichiometries (Luger *et al.* 1997; Andrews and Luger 2011; Grover *et al.* 2018), and many genomic processes are sensitive to perturbations in subunit stoichiometry within these complexes. For instance, disrupting the stoichiometric balance between H2A:H2B dimers and H3:H4 dimers in yeast causes genome instability and mitotic chromosome loss (Meeks-Wagner and Hartwell 1986). In all the genotypes, we assessed that display mutant phenotypes indicative of impaired Polycomb repression, the balance between *H3.2* and *H3.3* gene copy number is altered, and this change in the relative abundance of H3.2 and H3.3 could impact genome regulation. Consistent with this interpretation, work done in mice shows that displacement of H3.3—and enrichment of replication dependent H3.1—at regulatory regions causes transcriptional deregulation and chromosomal aberrations (Chen *et al.* 2020). Thus, the stoichiometric balance between H3.2 and H3.3 in chromatin may be critical for maintaining Polycomb target gene repression in flies.

A corollary to this model is that proper stoichiometric balance between H3 proteins and their chaperones is needed for repression of Polycomb targets. Previous work in mouse cells shows that H3.3-specific chaperones interact with PRC1 and PRC2, and that these interactions are needed for the recruitment of H3.3 to H3K9me3-dependent heterochromatin and for the establishment of H3K27me3 at developmental gene promoters (Banaszynski *et al.* 2013; Liu *et al.* 2020). Therefore, one could posit that altering the stoichiometric balance between H3.3 and its chaperones may perturb the establishment or maintenance of Polycomb domains. Notably, in our genetic screen for viability we identified Yem, an H3.3-specific chaperone, suggesting that mechanisms regulating the levels of canonical and variant histone within the genome involve control of histone deposition into chromatin.

Distinct roles of canonical *H3.2* and variant *H3.3* in Polycomb-mediated gene repression

Canonical *H3.2* and variant *H3.3* differ in their expression patterns and protein sequence. Our genetic analyses demonstrate that

Table 2. Chromosome 3L deficiency alleles tested for changes in viability.

Number[a]	Deficiency	Start coordinate[b]	End coordinate[b]	P value[c]
54	*Df(3L)ED50002*	22947	128631	-
23	*Df(3L)BSC362*	306168	628171	-
59	*Df(3L)Exel6085*	548528	749210	-
1♦	*Df(3L)ED4196*	639583	1478937	++
27	*Df(3L)BSC289*	1332329	1628100	-
41	*Df(3L)BSC800*	1628101	1647451	-
46	*Df(3L)BSC181*	1688724	1841694	-
64	*Df(3L)Aprt-32*	1795318	2555775	+
45	*Df(3L)ED4287*	1795442	2551761	-
22	*Df(3L)BSC119*	2600282	2823614	-
35	*Df(3L)Exel6092*	2821245	3047162	-
32	*Df(3L)BSC671*	2982129	3193143	-
14	*Df(3L)BSC672*	3081311	3206906	-
37	*Df(3L)ED4293*	3226338	3250564	-
60	*Df(3L)BSC368*	3759821	4040635	-
55	*Df(3L)BSC884*	5601375	5770185	-
34	*Df(3L)BSC410*	5763773	6483285	-
39	*Df(3L)BSC411*	5969060	6618726	-
19	*Df(3L)Exel6109*	6736213	6936639	-
53	*Df(3L)BSC27*	6936605	7136086	-
58	*Df(3L)BSC224*	6957557	7150109	-
50	*Df(3L)BSC33*	7242439	7350373	-
21	*Df(3L)BSC117*	7242575	7328086	-
30	*Df(3L)Exel8104*	7353086	7522363	-
13	*Df(3L)BSC375*	7510880	7904179	+
12	*Df(3L)BSC388*	7643513	8184286	-
63	*Df(3L)Exel6112*	8089573	8351924	-
56	*Df(3L)BSC815*	8256164	8499740	-
11	*Df(3L)BSC389*	8415284	8582696	+
16	*Df(3L)BSC816*	8632181	8738462	-
24	*Df(3L)ED4421*	8738426	9377175	-
47	*Df(3L)BSC113*	9342609	9416591	-
65	*Df(3L)AC1*	9351951	10140553	+
17	*Df(3L)BSC391*	9446770	9697191	-
26	*Df(3L)BSC118*	9508772	9690291	-
44	*Df(3L)BSC392*	9671802	9892354	-
15♦	*Df(3L)BSC673*	9756714	10174058	+
48	*Df(3L)BSC439*	10507047	10964106	-
20	*Df(3L)ED4470*	11090089	11826330	-
49	*Df(3L)ED4475*	11580140	12401701	-
38	*Df(3L)BSC730*	12156077	12836424	-
25	*Df(3L)BSC12*	13037536	13221789	-
18	*Df(3L)ED4543*	13928325	14751140	-
33	*Df(3L)BSC845*	15504128	15819023	-
51	*Df(3L)ED4606*	16080584	16773223	-
6	*Df(3L)ED4674*	16654384	17042518	+
7	*Df(3L)BSC414*	16962973	17469226	+
62	*Df(3L)Exel6132*	17414682	17526191	-
57	*Df(3L)ED4710*	17487463	18139299	-
5	*Df(3L)BSC775*	17788244	18891426	+
43	*Df(3L)BSC220*	18965662	19164368	-
8♦	*Df(3L)BSC839*	20313247	20486308	+
10	*Df(3L)BSC797*	20445923	20942833	-
31	*Df(3L)BSC449*	20850015	21196030	-
40	*Df(3L)BSC553*	20984731	21219092	-
3	*Df(3L)BSC419*	21218032	21597878	++
2	*Df(3L)BSC435*	21304739	21770618	++
36	*Df(3L)BSC836*	21382499	21497772	-
52	*Df(3L)BSC418*	21382499	21637924	-
9	*Df(3L)BSC223*	21909520	22078536	-
4♦	*Df(3L)BSC451*	22069194	22684788	++
42	*Df(3L)ED230*	22127751	22827471	-
29	*Df(3L)ED5017*	22828597	22991401	-
61	*Df(3L)1-16*	24292305	24536634	-
28	*Df(3L)6B-29*	24977118	25115180	-

[a] ♦ suggested haploinsufficiency.
[b] Breakpoints are as determined by the Bloomington stock center.
[c] +, $P < 0.05$; ++, $P < 0.01$. P-values obtained from a Chi-square test. See Supplementary Table 5 for P-values.

reducing *H3.3* gene copy number, but not *H3.2* gene copy number, causes a decrease in viability of *Pc* heterozygotes, suggesting *H3.2* and *H3.3* may have non-identical roles in Polycomb target gene regulation. $H3.3^4$ mutants do not uncouple *H3.2* expression from S phase, and *12xHWT* mutants still express *H3.3* throughout all of interphase. Thus, depleting the pool of H3 outside of S phase in the $H3.3^4$ mutants may sensitize cells to small perturbations in Polycomb-mediated gene repression during development. For example, Polycomb Response Elements (PREs), such as those that regulate *Ubx*, are sites of high histone turnover even though they reside within silent chromatin domains (Mito *et al.* 2007). As such, PREs may be particularly sensitive to the loss of available H3 protein outside of S phase. Reduced histone occupancy at PREs could impact Polycomb repression and organismal viability. Our finding that viability of animals with reduced *H3.2* gene copies increases as *H3.3* gene copy number increases supports this model. Alternatively, canonical H3.2 and variant H3.3 proteins may have distinct functions at PREs or Polycomb target domains. Consistent with this model, recent work in *D. melanogaster* shows that residue 36 on the N-terminal tail of H3.2 and H3.3 are both required for Polycomb-mediated repression but likely function through distinct mechanisms (Salzler *et al.* 2023). H3.2 and H3.3 differ at residue 31 on the N-terminal tail and H3.3S31 can be

Table 3. Decrease in *H3.2* and *H3.3* gene copy number increases frequency of ectopic sex combs.

Genotype	# H3.3 genes	# H3.2 genes	% legs with ectopic sex combs[a]
$H3.3B^{+/Y}$; $H3.3A^{+/+}$, $HisC^{+/+}$; $Df(3L)BSC419/+$	3	200	0%
$H3.3B^{+/Y}$; $H3.3A^{+/-}$, $HisC^{+/-}$; $Df(3L)BSC419/12xHWT$	2	112	15%●
$H3.3B^{+/Y}$; $H3.3A^{-/-}$, $HisC^{-/-}$; $Df(3L)BSC419/12xHWT$	1	12	40%●
$H3.3B^{+/Y}$; $H3.3A^{-/-}$, $HisC^{-/-}$; $+/12xHWT$	1	12	0%
$H3.3B^{+/Y}$; $H3.3A^{+/-}$, $HisC^{+/-}$; $Pc^3/12xHWT$	2	112	50%▲
$H3.3B^{+/Y}$; $H3.3A^{-/-}$, $HisC^{-/-}$; $Pc^3/12xHWT$	1	12	100%▲
$H3.3B^{+/Y}$; $H3.3A^{+/+}$, $HisC^{-/-}$; $+/12xHWT$	3	12	0%
$H3.3B^{+/Y}$; $H3.3A^{+/+}$, $HisC^{+/-}$; $Pc^3/12xHWT$	3	112	80%■
$H3.3B^{+/Y}$; $H3.3A^{+/+}$, $HisC^{-/-}$; $Pc^3/12xHWT$	3	12	100%■†
$H3.3B^{-/Y}$; $H3.3A^{-/-}$, $HisC^{+/+}$;	0	200	0%
$H3.3B^{+/Y}$; $H3.3A^{+/+}$, $HisC^{+/+}$; $Pc^3/+$	3	200	48%
$H3.3B^{+/Y}$; $H3.3A^{+/-}$, $HisC^{+/+}$; $Pc^3/+$	2	200	95%*
$H3.3B^{+/Y}$; $H3.3A^{-/-}$, $HisC^{+/+}$; $Pc^3/+$	1	200	96%*
$H3.3B^{-/Y}$; $H3.3A^{-/-}$, $HisC^{+/+}$; $Pc^3/+$	0	200	100%*

● Statistically significant difference in sex comb frequency between indicated genotype and $H3.3B^{+/Y}$; $H3.3A^{+/+}$, $HisC^{+/+}$; $Df(3L)BSC419/+$ ($P < 0.0001$).
▲ Statistically significant difference in sex comb frequency between indicated genotype and $H3.3B^{+/Y}$; $H3.3A^{-/-}$, $HisC^{-/-}$; $+/12xHWT$ ($P < 0.0001$).
■ Statistically significant difference in sex comb frequency between indicated genotype and $H3.3B^{+/Y}$; $H3.3A^{+/+}$, $HisC^{-/-}$; $+/12xHWT$ ($P < 0.0001$).
† Statistically significant difference in sex comb frequency between indicated genotype and $H3.3B^{+/Y}$; $H3.3A^{+/+}$; $HisC^{+/-}$; $Pc^3/12xHWT$ ($P < 0.0001$).
* Statistically significant difference in sex comb frequency between indicated genotype and $H3.3B^{+/Y}$; $H3.3A^{+/+}$, $HisC^{+/+}$; $Pc^3/+$ ($P < 0.0001$).
[a] P-values obtained from a Fisher's exact test. See Supplementary Table 7 for P-values.

phosphorylated (H3.3S31ph). It is known that histone H3 PTMs can influence one another (Yuan *et al.* 2011; Finogenova *et al.* 2020). Notably, H3.3S31ph affects the local PTM landscape and binding of factors that interact with the H3 tail, like the H3K36me3 reader ZMYND11 (Armache *et al.* 2020; Sitbon *et al.* 2020). Conceivably, these H3.3S31ph-specific effects on the PTM landscape could impact Polycomb function. Future studies probing the impacts of an H3.3S31A mutation, which renders the residue non-modifiable, on Polycomb function would address this possibility.

In summary, our data investigating the control of canonical and variant histone abundance provide evidence that Polycomb-mediated gene repression is sensitive to both canonical and variant histone gene copy number. This work advances our understanding of the distinct and overlapping functions of canonical and variant histones.

Data availability

Strains are available upon request. Raw RNA-seq data were deposited to Gene Expression Omnibus (GEO) under accession GSE228058. Additional information is available from the corresponding authors upon request.

Supplemental material available at GENETICS online.

Acknowledgements

The authors thank Aaron Crain for the generation of the *Df(2L) HisC^{Cadillac}* allele.

Funding

Conflicts of interest

The author(s) declare no conflict of interest.

Literature cited

Ahmad K, Henikoff S. The histone variant H3.3 marks active chromatin by replication-independent nucleosome assembly. Mol Cell. 2002;9(6):1191–1200. doi:10.1016/S1097-2765(02)00542-7.

Allis CD, Caparros ML, Jenuwein T, Reinberg D. Epigenetics. 2nd ed. Cold Spring Harbor, NY: Cold Spring Harbor Laboratory Press; 2015.

Andrews AJ, Luger K. Nucleosome structure(s) and stability: variations on a theme. Annu Rev Biophys. 2011;40(1):99–117. doi:10.1146/ANNUREV-BIOPHYS-042910-155329.

Armache A, Yang S, Martínez de Paz A, Robbins LE, Durmaz C, Cheong JQ, Ravishankar A, Daman AW, Ahimovic DJ, Klevorn T, *et al.* Histone H3.3 phosphorylation amplifies stimulation-induced transcription. Nature. 2020;583(7818):852–857. doi:10.1038/S41586-020-2533-0.

Bajusz I, Sipos L, Györgypál Z, Carrington EA, Jones RS, Gausz J, Gyurkovics H. The *Trithorax-mimic* allele of Enhancer of *zeste* renders active domains of target genes accessible to Polycomb-group-dependent silencing in *Drosophila melanogaster*. Genetics. 2001;159(3):1135–1150. doi:10.1093/GENETICS/159.3.1135.

Banaszynski LA, Wen D, Dewell S, Whitcomb SJ, Lin M, Diaz N, Elsässer SJ, Chapgier A, Goldberg AD, Canaani E, *et al.* Hira-dependent histone H3.3 deposition facilitates PRC2 recruitment at developmental loci in ES cells. Cell. 2013;155(1):107–120. doi:10.1016/j.cell.2013.08.061.

Berloco M, Fanti L, Breiling A, Orlando V, Pimpinelli S. The maternal effect gene, *abnormal oocyte (abo)*, of *Drosophila melanogaster* encodes a specific negative regulator of histones. Proc Natl Acad Sci U S A. 2001;98(21):12126–12131. doi:10.1073/pnas.211428798.

Blackledge NP, Klose RJ. The molecular principles of gene regulation by Polycomb repressive complexes. Nat Rev Mol Cell Biol. 2021; 22(12):815–833. doi:10.1038/s41580-021-00398-y.

Bonnet J, Boichenko I, Kalb R, Le Jeune M, Maltseva S, Pieropan M, Finkl K, Fierz B, Müller J. PR-DUB preserves Polycomb repression by preventing excessive accumulation of H2Aub1, an antagonist of chromatin compaction. Genes Dev. 2022;36(19–20):1046–1061. doi:10.1101/gad.350014.122.

Brown DT, Wellman SE, Sittman DB. Changes in the levels of three different classes of histone mRNA during murine erythroleukemia cell differentiation. Mol Cell Biol. 1985;5(11):2879–2886. doi:10.1128/mcb.5.11.2879.

Bulchand S, Menon SD, George SE, Chia W. Muscle wasted: a novel component of the *Drosophila* histone locus body required for muscle integrity. J Cell Sci. 2010;123(16):2697–2707. doi:10.1242/JCS.063172.

Chen D, Chen QY, Wang Z, Zhu Y, Kluz T, Tan W, Li J, Wu F, Fang L, Zhang X, *et al.* Polyadenylation of histone H3.1 mRNA promotes cell transformation by displacing H3.3 from gene regulatory elements. iScience. 2020;23(9):101518. doi:10.1016/J.ISCI.2020.101518.

Clark-Adams CD, Norris D, Osley MA, Fassler JS, Winston F. Changes in histone gene dosage alter transcription in yeast. Genes Dev. 1988;2(2):150–159. doi:10.1101/gad.2.2.150.

Cook RK, Christensen SJ, Deal JA, Coburn RA, Deal ME, Gresens JM, Kaufman TC, Cook KR. The generation of chromosomal deletions to provide extensive coverage and subdivision of the *Drosophila melanogaster* genome. Genome Biol. 2012;13(3):1–14. doi:10.1186/GB-2012-13-3-R21.

Dobin A, Davis CA, Schlesinger F, Drenkow J, Zaleski C, Jha S, Batut P, Chaisson M, Gingeras TR. STAR: ultrafast universal RNA-seq aligner. Bioinformatics. 2013;29(1):15–21. doi:10.1093/BIOINFORMATICS/BTS635.

Duronio RJ, Marzluff WF. Coordinating cell cycle-regulated histone gene expression through assembly and function of the histone locus body. RNA Biol. 2017;14(6):726–738. doi:10.1080/15476286.2016.1265198.

Eriksson PR, Ganguli D, Nagarajavel V, Clark DJ. Regulation of histone gene expression in budding yeast. Genetics. 2012;191(1):7–20. doi:10.1534/GENETICS.112.140145.

Finogenova K. Structural basis for PRC2 decoding of active histone methylation marks H3K36me2/3. elife. 2020;9:e61964:1–30. doi:10.7554/ELIFE.61964

Franklin S, Zweidler A. Non-allelic variants of histones 2a, 2b and 3 in mammals. Nature. 1977;266(5599):273–275. doi:10.1038/266273A0.

Goldberg AD, Banaszynski LA, Noh KM, Lewis PW, Elsaesser SJ, Stadler S, Dewell S, Law M, Guo X, Li X, *et al.* Distinct factors control histone variant H3.3 localization at specific genomic regions. Cell. 2010;140(5):678–691. doi:10.1016/j.cell.2010.01.003.

Gossett AJ, Lieb JD. *In vivo* effects of histone H3 depletion on nucleosome occupancy and position in *Saccharomyces cerevisiae*.

PLoS Genet. 2012;8(6):e1002771. doi:10.1371/JOURNAL.PGEN.1002771.

Grover P, Asa JS, Campos EI. H3–H4 histone chaperone pathways. Annu Rev Genet. 2018;52(1):109–130. doi:10.1146/annurev-genet-120417-031547.

Gruszka DT, Xie S, Kimura H, Yardimci H. Single-molecule imaging reveals control of parental histone recycling by free histones during DNA replication. Sci Adv. 2020;6(38):eabc0330. doi:10.1126/sciadv.abc0330.

Günesdogan U, Jäckle H, Herzig A. A genetic system to assess in vivo the functions of histones and histone modifications in higher eukaryotes. EMBO Rep. 2010;11(10):772–776. doi:10.1038/embor.2010.124.

Gunjan A, Verreault A. A Rad53 kinase-dependent surveillance mechanism that regulates histone protein levels in S. cerevisiae. Cell. 2003;115(5):537–549. doi:10.1016/S0092-8674(03)00896-1.

Hake SB, Garcia BA, Kauer M, Baker SP, Shabanowitz J, Hunt DF, Allis CD. Serine 31 phosphorylation of histone variant H3.3 is specific to regions bordering centromeres in metaphase chromosomes. Proc Natl Acad Sci U S A. 2005;102(18):6344–6349. doi:10.1073/pnas.0502413102.

Han M, Chang M, Kim UJ, Grunstein M. Histone H2B repression causes cell-cycle-specific arrest in yeast: effects on chromosomal segregation, replication, and transcription. Cell. 1987;48(4):589–597. doi:10.1016/0092-8674(87)90237-6.

Harris ME, Böhni R, Schneiderman MH, Ramamurthy L, Schümperli D, Marzluff WF. Regulation of histone mRNA in the unperturbed cell cycle: evidence suggesting control at two posttranscriptional steps. Mol Cell Biol. 1991;11(5):2416–2424. doi:10.1128/MCB.11.5.2416-2424.1991.

Hödl M, Basler K. Transcription in the absence of histone H3.2 and H3K4 methylation. Curr Biol. 2012;22(23):2253–2257. doi:10.1016/j.cub.2012.10.008.

Jang CW, Shibata Y, Starmer J, Yee D, Magnuson T. Histone H3.3 maintains genome integrity during mammalian development. Genes Dev. 2015;29(13):1377–1392. doi:10.1101/gad.264150.115.

Kassis JA, Kennison JA, Tamkun JW. Polycomb and trithorax group genes in Drosophila. Genetics. 2017;206(4):1699–1725. doi:10.1534/GENETICS.115.185116.

Kaufman TC, Lewis R, Wakimoto B. Cytogenetic analysis of chromosome 3 in Drosophila melanogaster: the homoeotic gene complex in polytene chromosome interval 84A-B. Genetics. 1980;94(1):115–133. doi:10.1093/GENETICS/94.1.115.

Kaygun H, Marzluff WF. Regulated degradation of replication-dependent histone mRNAs requires both ATR and Upf1. Nat Struct Mol Biol. 2005;12(9):794–800. doi:10.1038/NSMB972.

Kennison JA, Tamkun JW. Dosage-dependent modifiers of Polycomb and Antennapedia mutations in Drosophila. Proc Natl Acad Sci U S A. 1988;85(21):8136–8140. doi:10.1073/pnas.85.21.8136.

King HW, Fursova NA, Blackledge NP, Klose RJ. Polycomb repressive complex 1 shapes the nucleosome landscape but not accessibility at target genes. Genome Res. 2018;28(10):1494–1507. doi:10.1101/GR.237180.118.

Kornberg RD, Lorch Y. Primary role of the nucleosome. Mol Cell. 2020;79(3):371–375. doi:10.1016/J.MOLCEL.2020.07.020.

Lewis PW, Elsaesser SJ, Noh K-M, Stadler SC, Allis CD. Daxx is an H3.3-specific histone chaperone and cooperates with ATRX in replication-independent chromatin assembly at telomeres. Proc Natl Acad Sci U S A. 2010;107(32): 14075–14080. doi:10.1073/pnas.1008850107/-/DCSupplemental.

Li Z, Johnson MR, Ke Z, Chen L, Welte MA. Drosophila lipid droplets buffer the H2Av supply to protect early embryonic development. Curr Biol. 2014;24(13):1485–1491. doi:10.1016/J.CUB.2014.05.022.

Liao Y, Smyth GK, Shi W. featureCounts: an efficient general purpose program for assigning sequence reads to genomic features. Bioinformatics. 2014;30(7):923–930. doi:10.1093/BIOINFORMATICS/BTT656.

Lifton RP, Goldberg ML, Karp RW, Hogness DS. The organization of the histone genes in Drosophila melanogaster: functional and evolutionary implications. Cold Spring Harb Symp Quant Biol. 1977;42(0):1047–1051. doi:10.1101/sqb.1978.042.01.105.

Liu Z, Tardat M, Gill ME, Royo H, Thierry R, Ozonov EA, Peters AH. SUMOylated PRC1 controls histone H3.3 deposition and genome integrity of embryonic heterochromatin. EMBO J. 2020;39(13):e103697. doi:10.15252/EMBJ.2019103697.

Love MI, Huber W, Anders S. Moderated estimation of fold change and dispersion for RNA-seq data with DESeq2. Genome Biol. 2014;15(12):1–21. doi:10.1186/S13059-014-0550-8.

Loyola A, Almouzni G. Marking histone H3 variants: how, when and why? Trends Biochem Sci. 2007;32(9):425–433. doi:10.1016/J.TIBS.2007.08.004.

Luger K, Mäder A, Richmond R, Nature DS. Crystal structure of the nucleosome core particle at 2.8 Å resolution. Nature. 1997;389(6648):251–260. doi:10.1038/38444.

Malik HS, Henikoff S. Phylogenomics of the nucleosome. Nat Struct Biol. 2003;10(11):882–891. doi:10.1038/nsb996.

Martire S, Banaszynski LA. The roles of histone variants in fine-tuning chromatin organization and function. Nat Rev Mol Cell Biol. 2020;21(9):1–20. doi:10.1038/s41580-020-0262-8

Martire S, Gogate AA, Whitmill A, Tafessu A, Nguyen J, Teng YC, Tastemel M, Banaszynski LA. Phosphorylation of histone H3.3 at serine 31 promotes p300 activity and enhancer acetylation. Nat Genet. 2019;51(6):941–946. doi:10.1038/s41588-019-0428-5.

Marzluff WF, Duronio RJ. Histone mRNA expression: multiple levels of cell cycle regulation and important developmental consequences. Curr Opin Cell Biol. 2002;14(6):692–699. doi:10.1016/S0955-0674(02)00387-3.

Marzluff WF, Gongidi P, Woods KR, Jin J, Maltais LJ. The human and mouse replication-dependent histone genes. Genomics. 2002;80(5):487–498. doi:10.1006/GENO.2002.6850.

Maze I, Wenderski W, Noh K-M, Bagot RC, Tzavaras N, Purushothaman I, Elsässer SJ, Guo Y, Ionete C, Hurd YL, et al. Critical role of histone turnover in neuronal transcription and plasticity. Neuron. 2015;87(1):77–94. doi:10.1016/J.NEURON.2015.06.014.

McKay DJ, Klusza S, Penke TJR, Meers MP, Curry KP, McDaniel SL, Malek PY, Cooper SW, Tatomer DC, Lieb JD, et al. Interrogating the function of metazoan histones using engineered gene clusters. Dev Cell. 2015;32(3):373–386. doi:10.1016/J.DEVCEL.2014.12.025.

McKittrick E, Gafken PR, Ahmad K, Henikoff S. Histone H3.3 is enriched in covalent modifications associated with active chromatin. Proc Natl Acad Sci U S A. 2004;101(6):1525–1530. doi:10.1073/pnas.0308092100.

Meeks-Wagner D, Hartwell LH. Normal stoichiometry of histone dimer sets is necessary for high fidelity of mitotic chromosome transmission. Cell. 1986;44(1):43–52. doi:10.1016/0092-8674(86)90483-6.

Mito Y, Henikoff JG, Henikoff S. Genome-scale profiling of histone H3.3 replacement patterns. Nat Genet. 2005;37(10):1090–1097. doi:10.1038/ng1637.

Mito Y, Henikoff JG, Henikoff S. Histone replacement marks the boundaries of cis-regulatory domains. Science. 2007;315(5817):1408–1411. doi:10.1126/science.1134004.

Moore GD, Procunier JD, Cross DP, Grigliatti TA. Histone gene deficiencies and position-effect variegation in Drosophila. Nature. 1979;282(5736):312–314. doi:10.1038/282312a0.

Moore GD, Sinclair DA, Grigliatti TA. Histone gene multiplicity and position effect variegation in *Drosophila melanogaster*. Genetics. 1983;105(2):327–344. doi:10.1093/genetics/105.2.327.

Mühlen D, Li X, Dovgusha O, Jäckle H, Günesdogan U. Recycling of parental histones preserves the epigenetic landscape during embryonic development. Sci Adv. 2023;9(5):eadd6440. doi:10.1126/SCIADV.ADD6440.

Myung K, Pennaneach V, Kats ES, Kolodner RD. *Saccharomyces cerevisiae* chromatin-assembly factors that act during DNA replication function in the maintenance of genome stability. Proc Natl Acad Sci U S A. 2003;100(11):6640–6645. doi:10.1073/PNAS.1232239100.

Nashun B, Hill PWS, Smallwood SA, Dharmalingam G, Amouroux R, Clark SJ, Sharma V, Ndjetehe E, Pelczar P, Festenstein RJ, *et al.* Continuous histone replacement by Hira is essential for normal transcriptional regulation and de novo DNA methylation during mouse oogenesis. Mol Cell. 2015;60(4):611–625. doi:10.1016/j.molcel.2015.10.010.

Nelson DM, Ye X, Hall C, Santos H, Ma T, Kao GD, Yen TJ, Harper JW, Adams PD. Coupling of DNA synthesis and histone synthesis in S phase independent of cyclin/cdk2 activity. Mol Cell Biol. 2002; 22(21):7459–7472. doi:10.1128/MCB.22.21.7459-7472.2002.

Orlando V. Polycomb, epigenomes, and control of cell identity. Cell. 2003;112(5):599–606. doi:10.1016/S0092-8674(03)00157-0.

Orsi GA, Algazeery A, Meyer RE, Capri M, Sapey-Triomphe LM, Horard B, Gruffat H, Couble P, Aït-Ahmed O, Loppin B. *Drosophila* Yemanuclein and HIRA cooperate for de novo assembly of H3.3-containing nucleosomes in the male pronucleus. PLoS Genet. 2013;9(2):e1003285. doi:10.1371/journal.pgen.1003285.

Pantazis P, Bonner WM. Specific alterations in the pattern of histone-3 synthesis during conversion of human leukemic cells to terminally differentiated cells in culture. Differentiation. 1984;28(2):186–190. doi:10.1111/j.1432-0436.1984.tb00282.x.

Paro R. Imprinting a determined state into the chromatin of *Drosophila*. Trends Genet. 1990;6(12):416–421. doi:10.1016/0168-9525(90)90303-N.

Pattatucci AM, Otteson DC, Kaufman TC. A functional and structural analysis of the *Sex combs reduced* locus of *Drosophila melanogaster*. Genetics. 1991;129(2):423–441. doi:10.1093/GENETICS/129.2.423.

Piña B, Suau P. Changes in histones H2A and H3 variant composition in differentiating and mature rat brain cortical neurons. Dev Biol. 1987;123(1):51–58. doi:10.1016/0012-1606(87)90426-X.

Rai TS, Puri A, McBryan T, Hoffman J, Tang Y, Pchelintsev NA, van Tuyn J, Marmorstein R, Schultz DC, Adams PD. Human CABIN1 is a functional member of the human HIRA/UBN1/ASF1a histone H3.3 chaperone complex. Mol Cell Biol. 2011;31(19):4107–4118. doi:10.1128/MCB.05546-11.

Ray-Gallet D, Ricketts MD, Sato Y, Gupta K, Boyarchuk E, Senda T, Marmorstein R, Almouzni G. Functional activity of the H3.3 histone chaperone complex HIRA requires trimerization of the HIRA subunit. Nat Commun. 2018;9(1):3103. doi:10.1038/s41467-018-05581-y.

Roote J, Russell S. Toward a complete *Drosophila* deficiency kit. Genome Biol. 2012;13(3):149. doi:10.1186/GB-2012-13-3-149.

Sakai A, Schwartz BE, Goldstein S, Ahmad K. Transcriptional and developmental functions of the H3.3 histone variant in *Drosophila*. Curr Biol. 2009;19(21):1816–1820. doi:10.1016/j.cub.2009.09.021.

Salzler HR, Vandadi V, McMichael BD, Brown JC, Boerma SA, Leatham-Jensen MP, Adams KM, Meers MP, Simon JM, Duronio RJ, *et al.* Distinct roles for canonical and variant histone H3 lysine-36 in Polycomb silencing. Sci Adv. 2023;9(9):eadf2451. doi:10.1126/SCIADV.ADF2451.

Sauer P, Gu Y, Liu WH, Mattiroli F, Panne D, Luger K, Churchill M. Mechanistic insights into histone deposition and nucleosome assembly by the chromatin assembly factor-1. Nucleic Acids Res. 2018;46(19):9907–9917. doi:10.1093/NAR/GKY823.

Schneiderman JI, Sakai A, Goldstein S, Ahmad K. The XNP remodeler targets dynamic chromatin in *Drosophila*. Proc Natl Acad Sci U S A. 2009;106(34):14472–14477. doi:10.1073/pnas.0905816106.

Shibahara KI, Stillman B. Replication-dependent marking of DNA by PCNA facilitates CAF-1-coupled inheritance of chromatin. Cell. 1999;96(4):575–585. doi:10.1016/S0092-8674(00)80661-3.

Sinclair DAR, Mottus RC, Grigliatti TA. Genes which suppress position-effect variegation in *Drosophila melanogaster* are clustered. Mol Gen Genet. 1983;191(2):326–333. doi:10.1007/BF00334834.

Singh RK, Kabbaj MHM, Paik J, Gunjan A. Histone levels are regulated by phosphorylation and ubiquitylation-dependent proteolysis. Nat Cell Biol. 2009;11(8):925–933. doi:10.1038/NCB1903.

Sitbon D, Boyarchuk E, Dingli F, Loew D, Almouzni G. Histone variant H3.3 residue S31 is essential for *Xenopus* gastrulation regardless of the deposition pathway. Nat Commun. 2020;11(1):1–15. doi:10.1038/s41467-020-15084-4.

Smith AV, King JA, Orr-Weaver TL. Identification of genomic regions required for DNA replication during Drosophila embryogenesis. Genetics. 1993;135(3):817–829. doi:10.1093/GENETICS/135.3.817.

Smith MM, Murray K. Yeast H3 and H4 histone messenger RNAs are transcribed from two non-allelic gene sets. J Mol Biol. 1983;169(3): 641–661. doi:10.1016/S0022-2836(83)80163-6.

Smith S, Stillman B. Purification and characterization of CAF-I, a human cell factor required for chromatin assembly during DNA replication in vitro. Cell. 1989;58(1):15–25. doi:10.1016/0092-8674(89)90398-x.

Stephenson RA, Thomalla JM, Chen L, Kolkhof P, White RP, Beller M, Welte MA. Sequestration to lipid droplets promotes histone availability by preventing turnover of excess histones. Development. 2021;148(15):dev199381. doi:10.1242/DEV.199381/270998/AM/SEQUESTRATION-TO-LIPID-DROPLETS-PROMOTES-HISTONE.

Sullivan E, Santiago C, Parker ED, Dominski Z, Yang X, Lanzotti DJ, Ingledue TC, Marzluff WF, Duronio RJ. *Drosophila* stem loop binding protein coordinates accumulation of mature histone mRNA with cell cycle progression. Genes Dev. 2001;15(2):173–187. doi:10.1101/gad.862801.

Szenker E, Ray-Gallet D, Almouzni G. The double face of the histone variant H3.3. Cell Res. 2011;21(3):421–434. doi:10.1038/cr.2011.14.

Tagami H, Ray-Gallet D, Almouzni G, Nakatani Y. Histone H3.1 and H3.3 complexes mediate nucleosome assembly pathways dependent or independent of DNA synthesis. Cell. 2004;116(1): 51–61. doi:10.1016/S0092-8674(03)01064-X.

Torné J, Ray-Gallet D, Boyarchuk E, Garnier M, Le Baccon P, Coulon A, Orsi GA, Almouzni G. Two HIRA-dependent pathways mediate H3.3 de novo deposition and recycling during transcription. Nat Struct Mol Biol. 2020;27(11):1057–1068. doi:10.1038/s41594-020-0492-7.

Tvardovskiy A, Schwämmle V, Kempf SJ, Rogowska-Wrzesinska A, Jensen ON. Accumulation of histone variant H3.3 with age is associated with profound changes in the histone methylation landscape. Nucleic Acids Res. 2017;45(16):9272–9289. doi:10.1093/nar/gkx696.

Urban MK, Zweidler A. Changes in nucleosomal core histone variants during chicken development and maturation. Dev Biol. 1983;95(2):421–428. doi:10.1016/0012-1606(83)90043-X.

Verreault A, Kaufman PD, Kobayashi R, Stillman B. Nucleosome assembly by a complex of CAF-1 and acetylated histones H3/H4. Cell. 1996;87(1):95–104. doi:10.1016/S0092-8674(00)81326-4.

Wirbelauer C, Bell O, Schübeler D. Variant histone H3.3 is deposited at sites of nucleosomal displacement throughout transcribed genes while active histone modifications show a promoter-proximal bias. Genes Dev. 2005;19(15):1761–1766. doi:10.1101/gad.347705.

Wunsch AM, Lough J. Modulation of histone H3 variant synthesis during the myoblast-myotube transition of chicken myogenesis. Dev Biol. 1987;119(1):94–99. doi:10.1016/0012-1606(87)90210-7.

Ye X, Franco AA, Santos H, Nelson DM, Kaufman PD, Adams PD. Defective S phase chromatin assembly causes DNA damage, activation of the S phase checkpoint, and S phase arrest. Mol Cell. 2003;11(2):341–351. doi:10.1016/S1097-2765(03)00037-6.

Yuan W, Xu M, Huang C, Liu N, Chen S, Zhu B. H3k36 methylation antagonizes PRC2-mediated H3K27 methylation. J Biol Chem. 2011; 286(10):7983–7989. doi:10.1074/JBC.M110.194027.

Zweidler A. Core histone variants of the mouse: primary structure and differential expression. Wiley New York; 1984.

Editor: P. Geyer